APPENDIX A

The Current State of Knowledge

A.1 INTRODUCTION

Interlayer systems have received considerable attention in recent years as viable solutions to enhance pavement performance. The introduction of these systems to the transportation field was mainly due to the unsatisfactory performance of traditional materials exposed to a dramatic increase and change in traffic patterns; a need that still exists. The fast deterioration of the highway systems constructed during the 1950s and 1960s also contributed to the need for a more effective rehabilitation methodology (Barksdale 1991). The use of interlayer systems is not new, however. Beginning in the early 1930's, Beckham and Mills suggested the use of cotton fibers as an interlayer system in flexible pavement in South and North Carolina (Beckham et al. 1935). Nowadays, the use of degradable material, such as cotton fibers, may not be the best alternative for reinforcement, but the concept remains the same.

Although it is generally recognized that each interlayer should be used for a specific goal, and that not all interlayers have a strengthening function, it is not widely understood that interlayers may negatively impact pavement performance if they are not properly used. Moreover, surveys have shown that field engineers tend to believe that any interface products can improve pavement performance, regardless of their contribution mechanisms (Francken 1993). This oversimplified view of the situation has led to contradictory experiences and opinions about the benefits of these materials. While some studies emphasize the surplus advantages, such as substantial savings in hot-mix asphalt (HMA) thickness (Kennepohl et al. 1985), others found that interlayer systems are "useless" (Donna 1993). Moreover, reinforced sections required more maintenance than non-reinforced ones. This contradiction is mainly due to the gap between in-situ performance and the understanding of the contributing mechanism. In

general, interlayer products are thought to provide five distinct functions (an interlayer system may provide one or more of these functions):

1. **Separation**, by preventing the intrusion of fines from the subgrade into the base layer under the influence of traffic loads.
2. **Filtering,** by preventing fine particles being washed from the subgrade into the road base due to the action of water.
3. **Reinforcement,** by improving the tensile strength of a pavement layer and spreading the load over a larger area.
4. **Moisture Barrier,** by abating water infiltration to the underneath pavement layers, protecting them from the detrimental effects of water.
5. **Stress Relief,** by allowing for larger deformations in the interlayer, which may dissipate the excess amount of energy that would otherwise increase the rate of crack propagation.

The behavior mechanism involved in each function is different. Some characteristics and properties are specifically required in the interlayer to achieve the seeking function. Prior to describing each type of interlayer system, it is essential to present the current state of knowledge on the behavior mechanisms of interlayer systems.

A.2 BEHAVIOR MECHANISM

The behavior mechanisms involved in the five aforementioned functions depends on different factors that influence the success of the interlayer product. The contributing mechanisms involved in the separation, filtration, and infiltration-reduction functions are self-explanatory. Whether the benefits of these three functions have been verified or quantified will be discussed in the following sections. On the other hand, the behavior mechanism involved in the stress-relief and reinforcement functions are far more complex, and will be explained in detail.

A.2.1 Separation

Two mechanisms may significantly reduce the thickness of the installed base layer when constructed over a soft subgrade (Bhutta 1998):

a. The pumping of the subgrade fines into the base course aggregate voids as excess pore water pressures dissipate due to dynamic vehicular loading. This process reduces the particle-to-particle contact, decreasing the aggregate's stability and strength.
b. The penetration of aggregate stone particles into soft subgrade soil**,** as local shear failure of the soil may occur.

When functioning as a separation layer, an interlayer (usually a geotextile) prevents aggregate base grains from being pressed out of the base into the soft subgrade, and also prevents the intrusions of fines from the subgrade into the base layer due to dynamic vehicular loading.

A.2.2 Filtration

The filtration function is closely related to the separation function. In this case, an interlayer system, usually a geotextile, prevents fine particles being washed from the subgrade into the base or subbase layer under the action of water and repetitive moving load.

A.2.3 Moisture Barrier

The primary source of moisture in pavement structures is rainwater, which becomes a major source of failure if not adequately drained. An effective moisture barrier interlayer, usually a geomembrane or geotextile, can prevent the saturation of underlying layers and force the water to drain laterally to a shoulder drain system, given that the water table level is low. The effectiveness of the interlayer as a moisture barrier mainly

depends on the interface staying intact after installation, which is not always the case, especially in overlay applications (Chen and Frederick 1992).

A.2.4 Reinforcement

The term "*reinforcement*" refers to the ability of an interlayer to better distribute the applied load over a larger area, compensating for a lack of tensile strength within the pavement materials. As in any reinforcement applications, the reinforcing material should be stiffer than the material to be reinforced (Rigo 1993). Two areas of reinforcing produce a great deal of success in pavement applications: subgrade and granular layer reinforcement, and HMA layer and overlay reinforcement.

A.2.4.1 Reinforcement of Subgrade and Granular Layers

The effectiveness of the reinforcement of the subgrade and granular layers depends on three contributing mechanisms:

- Bonding between the reinforcement and the surrounding pavement materials defines the mobilized portion of the interlayer strength that may contribute to the reinforcement. This mechanism is essential for a solid interlayer (e.g. geotextile).
- Interlocking between the reinforcement and the surrounding aggregates. This mechanism, which is essential for interlayer products with openings, results from the protrusion of aggregates through the openings of the interlayer (Hozayen et al. 1993).
- Confinement of the reinforced layer results in a reduction of the horizontal deformation by lateral restraint. This mechanism is particularly important with subgrade soils that are not too weak (Zanten 1986).

A.2.4.2 Reinforcement of HMA layers and overlays

With an increase in rehabilitation funds and a decline in new road construction, this type of reinforcement appears to be the major contribution that interlayers products may provide in pavement applications. Repairing a deteriorated road using a conventional overlay is rarely a lasting solution. The original cracks, which move due to thermal and traffic loadings, reflect in the new surface, causing "reflection cracking" (Steen 2000). Different methods, including the use of interlayer systems, have been suggested. The general belief among pavement engineers is that, even when a technique to delay reflective cracking is successful, the cost is equivalent to the cost of repairing the cracks (Huges et al. 1973). This opinion appears misleading if we consider the appearance of the reflection cracking a few months after application of the overlay, which is sometimes the case.

According to Lytton, the passing of a wheel load over a crack in the existing pavement causes three critical pulses, one maximum bending and two maximum shear stresses (Lytton 1989). As the movement of the crack increases, the propagation of the crack to the overlay occurs faster. A difference in temperature can also contribute to the crack propagation. Contraction and curling of the old pavement caused by temperature variation may result in the opening of the cracks, which may induce horizontal stresses in the HMA overlay.

Based upon earlier work by Lytton and Monismith, the reinforcement mechanism seems to be better understood, with major outlines drawn for the requirements from an interlayer system to act as reinforcement (Lytton 1989; Monismith and Coetzee 1980). Button and Lytton summarized the reinforcement failure mode as follows (Button et al. 1987):

- The crack starts to propagate (due to thermal and traffic loading) from its original position upward until it reaches the reinforcement layer. If the interlayer is stiff enough, the crack will turn laterally and moves along the interface until its energy is exhausted. Lytton noted that the reinforcement failure would develop only after debonding has occurred between the lower layer and the interlayer (Lytton 1989).

- From the previous mechanism, it can be concluded that reinforcement can only occur if the interlayer is sufficiently thick and is stiffer than the surrounding materials. The stiffness of an interface is equal to the material elastic modulus times its thickness (Barksdale 1991).
- Based on the explained mechanism, a reinforcement interface may contribute to the structural capacity of the pavement. Given this, it is realistic to reduce the required thickness to reach the same level of performance. The amount of reduction is still mainly based on empirical rules and individual experiences.

A.2.5 Stress Relief

A stress relief interlayer is a soft layer that is usually placed at the bottom of an HMA overlay to absorb a large portion of the energy, which would otherwise be part of the crack propagation process (Barksdale 1991). Based on earlier work by Lytton and Monismith, the stress relief failure mode can be summarized as follows (Lytton 1989):

- The crack starts to propagate (due to thermal and traffic loading) from its original position upward until it reaches the stress-relieving layer. Due to its low stiffness, the interlayer will exhibit large deformations, which will be accompanied with a dissipation of energy. The crack propagation will stop for a while due to the lack of energy, and then propagate from the top of the interlayer upward to the surface.
- A second mode of failure was hypothesized by Lytton based on laboratory results, but was not supported by any other studies. In this failure mode, the crack starts to propagate from its original position upward until it reaches the stress-relieving layer. The crack then begins from the top of the overlay to the interlayer.
- It is clear from the explained mechanism that a low stiffness interlayer product is preferred in this application. In this case, the interlayer product will only retard the appearance of the reflection cracking.

Monismith and Coetzee (1980) associated the contribution of a stress-relief interlayer to the pavement system with what they called “a crack arrest” phenomenon. Based on this

mechanism, a soft interlayer is capable of redirecting the crack from its original direction to the horizontal plane. This phenomenon was also noticed by Majidzadeh (1976) when testing HMA beam reinforced at mid depth with "Petromat." However, it was reported that the use of a stress-reliever interlayer may increase the chance of delamination between the overlay and the cracked HMA layer. It is clear from the explained mechanism that stress-relieving interlayers will not contribute to the structural capacity of the pavement, and it is misleading to talk about saving in layer thicknesses.

A.3 TYPES OF INTERLAYER SYSTEMS

Starting from the early 1960s, different interlayer products have been suggested, ranging from metallic grids to different types of geosynthetics. Table A-1 illustrates the major types of interlayer based on their application in pavement systems. The indicated price ranges does not include installation costs, and the need for a tack coat or slurry seal (if any). The following sections present a detailed presentation of each class of interlayer products.

A.3.1 Geosynthetics

"Geosynthetics" is the collective term applied to thin and flexible sheets of synthetic polymer material incorporated in soils, pavements, and bridge decks (Donovan et al. 2000). Geosynthetics are divided into six major categories (Koerner 1994):

a. Geotextiles: The most widely used type of geosynthetics (also called fabric). They are formed from permeable synthetic fibers that are weaved together to form a porous, flexible fabric.
b. Geogrids: made from high-density polypropylene or polyethylene with an open mesh structure that allows interlocking with the surrounding materials.
c. Geomembranes: made from impervious, very soft, thin sheets of rubber or plastic materials.

Table A-1. The Major Types of Interlayer Products

Interlayer Type	Picture	Applications	Estimated Cost ($/m^2)
Galvanized Steel Netting	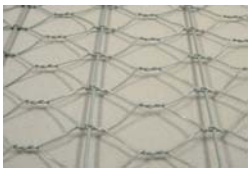	Reinforcement	3.50-6.00
Woven Geotextile		Separation Filtration	0.30-0.60
Geogrid		Reinforcement	3.50-5.50
Geonet		Drainage	2.30-2.50
Glass-Grid	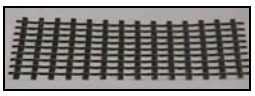	Reinforcement	5.50-7.00
Non-Woven Geotextile		Moisture Barrier Filtration Separation Stress Relief	0.75-1.25
Geocomposite		Moisture Barrier Stress Relief Separation	10.0-11.0

d. Geocells: cubic confinement cells made from slotted aluminum sheets or prefabricated polymeric systems. They are mainly used as soil confinement to improve the soil bearing capacity.
e. Geocomposites: a multi-purpose system consisting of two or more types of geosynthetics to achieve more than one function in the pavement system (e.g. water prevention and stress-relief).

For the past 30 years, geosynthetics have been used to provide the aforementioned five distinct functions (separation, filtration, reinforcement, stress relief, and pavement moisture barrier). Performances of geosynthetics have been mixed, and cannot be considered conclusive (Barksdale 1991). In some experimental studies, the use of geosynthetics has been successful (Halim et al. 1983); in other cases, poor performance was observed. Until now, the decision to use a given type of geosynthetics has been mainly based on field experiences and empirical rules. With the incredible growth of the geosynthetics market in pavement applications, more comprehensive studies are presented to better understand and explain geosynthetic behavior mechanism. Based on the reviewed literature, geosynthetics have been evaluated in the following applications.

A.3.1.1 Geosynthetics as Moisture Barrier

Paving fabrics have been tested as moisture barriers (Marienfeld et al. 1996; Al-Qadi et al. 1999). Although many laboratory studies emphasized the waterproofing benefits of paving fabrics (Smith 1984), there have been limited actual field quantification of these benefits.

The drainage capability of geosynthetics has long been a source of debate, as it has generally been impossible to verify. However, with advances in electromagnetic techniques, moisture monitoring using time-domain reflectometry (TDR) and ground-penetrating radar (GPR) appears more feasible. These new techniques appear to offer a reliable solution to verify paving fabric waterproofing benefits. In 1999, Al-Qadi et al. employed a ground-penetrating radar system to detect the presence of moisture beneath pavements. Although these offered promising results, a number of studies emphasized

that the use of geosynthetics as moisture barrier may not be cost effective, even where successful, as long as the detrimental effect of water is not quantifiable (Barksdale 1991).

A.3.1.2 Geosynthetics as Reinforcement for Base and Subgrade Layers

Geogrids and geotextiles have been tested as reinforcements for base and subbase layers. Based on laboratory testing, various studies showed that a geogrid-reinforced pavement could provide substantial savings in base thickness (Halim et al. 1983; Kennepohl et al. 1985; Barksdale et al. 1989; Al-Qadi et al. 1994). However, it seems that this conclusion was only drawn based on the cyclic circular plate-loading test. Based on field evaluation, Nejad and Small found that the use of geogrid could significantly reduce permanent deformation, especially when placed at the middle of the base layer (Nejad et al. 1996).

Cancelli et al. investigated the structural contribution of geogrid and geotextiles when placed between soft soil and a granular subbase (Cancelli et al. 1999). Based on the results obtained from a pavement full-scale facility, Cancelli found that geogrids are effective in reducing overall rutting when used to reinforce a very soft subgrade (CBR less than three percent). This conclusion represented the major trend in the results.

The effectiveness of geotextiles as a base or subbase reinforcement has been mixed among different investigators. Al-Qadi et al. found that a geotextile-reinforced section can withstand 1200 cycles, compared to 160 cycles for the non-reinforced section, to reach a 25.4mm vertical deformation (Al-Qadi et al. 1994). On the other hand, Barksdale et al. claimed that the use of a low stiffness geotextile is not likely to increase the overall stiffness of the pavement system (Barksdale et al. 1989). Based on this study, it was also found that a geogrid has the same reinforcing capability of a woven geotextile having a stiffness approximately 2.5 times as great as the geogrid. This finding may be explained by the ability of the geogrid to rely on the interlock and bonding mechanisms, while the geotextile can only contribute through the bonding and confinement mechanisms. Cancelli et al. found that high-strength woven geotextiles can provide good separation functions, but offer a limited reinforcement contribution (Cancelli et al. 1999).

A.3.1.3 Geosynthetics as Reinforcement for HMA Layers and Overlays

It was previously mentioned that, in order to act as reinforcement, an interlayer must have a stiffness equal to or greater than that of the surrounding materials. The only geosynthetic products that fulfill this condition are geogrids and glass-grids. Until now, the potential of these products as reinforcement has been inconclusive:

- Based on field evaluation, the Colorado Department of Transportation (CDOT) found that the use of glass-grid in road overlay is "completely useless" (Donna 1993). Moreover, it appeared that the reinforced sections might show more distresses than the unreinforced ones. The installation of the glass-grid was also reportedly very tedious.
- Based on laboratory results, Komatsu et al. claimed that geogrid-reinforced HMA showed "remarkable" performance when compared to unreinforced samples (Komatsu et al. 1998). In this study, the improvement in durability was found to increase with the decrease in geogrid-mesh size. This may be explained by the improved interlock between the grid and the surrounding material when the geogrid mesh openings become smaller.
- As part of the annual highway performance monitoring system (HPMS), two geogrid types were tested on Interstate Highway 10 (Steinberg 1992). Four rehabilitation techniques were compared on a single lane: two geogrid types (one heat sensitive, and the other with greater heat resistance) and two routine rehabilitation processes with a variety of overlay thicknesses. After three years of heavy traffic, the section incorporating the heat sensitive geogrid (requiring insulation from a seal coat) "failed shortly after traffic used that lane." The geogrid with greater heat resistance performed satisfactorily, but was not the best section.
- Steinberg also presented other states' experiences with geogrids (Steinberg 1992). The Minnesota Department of Transportation (MDOT) tested two glass-grid types and a geogrid. Both glass-grid types had installation problems. No paving problems occurred with the geogrid. However, the final evaluation of the geogrid

concluded that this interlayer is not suitable for large-scale projects because of the tensioning operation required during installation. The New Mexico State Highway and Transportation Department (NMSHT) also tested both geogrid and glass-grid interlayers. A slight improvement was noticed for the geogrid sections, but it seems that the installation caused major delays.

A.3.1.4 Geosynthetics as Stress-Relief Interlayers

The stress-relief mechanism is desirable when an overlay is applied to a deteriorated existing pavement. If installed properly, the interlayer will change the energy balance at the crack tip by allowing for larger strain energy dissipation. To properly contribute to the pavement system as a stress reliever, it was shown that the interlayer should have a lower stiffness than the surrounding materials. It was emphasized that a stress-relieving interlayer is not a substitute for the overlay structural capacity. The main role of a stress-relieving interlayer is to delay the reflection of the original cracks to the surface. A low strength woven or non-woven geotextile and a geocomposite membrane all have a low stiffness. Therefore, their use as stress-relievers is feasible. However, only limited experiences with geosynthetics as stress-relievers have been documented to date.

Chen and Frederick investigated the effectiveness of non-woven geotextiles as stress-relieving interlayers when installed prior to an overlay (Chen and Frederick 1992). Two techniques were investigated: full-lane width application and geotextile strips over single cracks. The strip application "failed within the first year and should not be considered for future evaluations" (Chen and Frederick 1992). In the full-lane width application, the sections with geotextile performed better than the ones without geotextile: The interlayer treatment resulted in a three-year increase in the service life of the overlay. However, based on life cycle cost analysis, interlayer treatments were not cost effective when compared to normal overlays.

Carmichael and Marienfeld reviewed and synthesized the existing literature on the use of paving fabrics in enhancing the performance of HMA overlays over existing flexible or rigid pavement systems (Carmichael and Marienfeld 1999). Over 200 reports on the use of nonwoven paving fabrics were reviewed, and 50 experts were interviewed.

The use of nonwoven paving fabrics in enhancing the performance of HMA overlays were divided into four distinct applications:

- Paving fabric with a chip seal over an existing subgrade or unbound base layers;
- Paving fabric with a chip seal over an existing flexible pavement;
- Paving fabric over an existing flexible pavement; and
- Paving fabric over an existing rigid pavement.

Carmichael and Marienfeld identified two major benefits of the interlayer system when used in these applications: control of moisture infiltration to the pavement layers and delay of the reflection of existing cracks and joints. In general, based on the observed performance in over 50 different test sites, it was concluded that the use of nonwoven paving fabrics is successful in these applications. As an example, the results of a test site in France were reported, where similar sections with and without geotextile were compared. After ten years in service, the control section exhibited 65% reflection cracking, while the fabric section showed 40% reflection cracking. Based on the reviewed literature and the interviewed experts, the authors concluded that the use of a paving fabric increases the overlay performance by a factor equivalent to 30.4 to 54.7 mm in overlay thickness, with an average performance equivalency of 33.0 mm. Although the detailed life-cycle cost analysis (LCCA) was not presented, it was based on the assumption that the cost of a nonwoven paving fabric in place is equivalent to the cost of 12.7mm of HMA overlay.

Buttlar et al. investigated the cost-effectiveness of paving fabrics in delaying the reflection of cracks based on the field performance of 52 test projects in the state of Illinois (Buttlar et al. 2000). All projects consisted of rigid pavement systems overlaid by multiple HMA layers over the life span of the structure. Both strip and area treatment rehabilitation strategies were investigated with consideration of eight replicates for each combination of treatment and climatic conditions. Some combinations were not available to complete the entire factorial design; the distribution of the 52 projects was 26 strip, 17 treatment areas, and nine control sections. Overall, while strip applications improved

pavement serviceability by 1.1 years, area applications improved pavement serviceability by 3.6 years.

A.3.2 Closure

Over the past twenty years, geosynthetics have occupied the major share in the market of interlayer systems. Unfortunately, the main reason behind this success was not directly related to performance, but rather to the surplus production of plastic. A growing amount of evidence indicates that a geosynthetic layer can provide a reinforcement benefit to the pavement system only when the geosynthetics have a modulus larger or equal to that of the surrounding material (e.g. geogrid) (Lytton 1989; Vanelstraete et al. 1993). Moreover, it was also recently concluded that a stress relief layer could not justify a reduction in the overlay thickness. These major findings question the cost-effectiveness of a geosynthetic interlayer if a significant enhancement of the performance is not expected, which has not been conclusively documented to date. More research and testing are needed before promoting a geosynthetic interlayer from an experimental product to a feasible solution.

A.3.3 Steel Reinforcement

A.3.3.1 Earlier Experiences with Welded Wire

One of the oldest interface systems used in flexible pavements is steel reinforcement. This technique, which appeared in the early 1950s, was based on the general concept that if HMA is strong in compression and weak in tension, then reinforcement could be used to provide needed resistance to tensile stresses (Busching et al. 1970). At that time, the idea might be taken from the very successful steel-reinforced Portland cement concrete (PCC). However, it appears that steel reinforcement was abandoned in the early 1970s after tremendous difficulties were encountered in its installation.

The process reemerged in the early 1980s with a new class of steel reinforcement products in Europe. Many of the earlier problems appeared to have been solved, and satisfactory experiences with the new class of steel reinforcement were reported

(Vanelstraete et al. 2000). To date, the new class of steel reinforcement has only been installed in the United States in a small number of experimental sections starting in 2001 (e.g. SR-180, Turnpike MP85-88, and SR3013, which are all located in the State of Pennsylvania). Prior to presenting information about current steel reinforcement techniques, the original experience with welded wire reinforcement is reviewed.

In a state-of-the-art review, Busching et al. presented several states' experiences with welded steel wire reinforcement in the period between 1950 and 1970 (Busching et al. 1970). Configurations of welded steel wire reinforcement included No. 10 wire in either 101.6 x 101.6 or 76.2 x 152.4-mm mesh. At that time, several states, including Minnesota, Michigan, Illinois, Wisconsin, New York, and Texas initiated experimental sections of highway that incorporated welded wire reinforcement. Their specific goal was to investigate its effectiveness in retarding the reflection of cracks in HMA overlays. Problems during installation were reported and summarized by Davis (Davis 1960). Transverse cracks at mesh splices were caused by the expansion and contraction of the mesh, which required an adequate overlap between the rolls. Buckling of the steel mesh, due to the movement of the paving equipment, and the possibility of resulting low density in the upper HMA layer were also noted. The mesh was also reported to rust, neck, and break at cracks.

In spite of its reported installation difficulties, welded steel mesh was found effective in retarding reflective cracks. Based on field evaluation in Toronto, steel-reinforcement had significantly reduced the appearance of reflection cracking after five years of service (Brownridge et al. 1964). Conclusions from other field evaluations included the following statement (Tons et al. 1960): "The cost of a 75 mm reinforced overlay was no greater than a 95 mm unreinforced overlay. However, the 95 mm unreinforced has a transverse crack incidence five times greater than the 75-mm reinforced." Busching identified several advantages that may result from reinforcement (Busching et al. 1970):

- Increased tensile and shear strength and resistance to cracking
- Coherence of the pavement even after cracking
- Increased resistance to fatigue failure and greater pavement flexibility

- Potential material savings and enhanced performance
- Increased resistance to flow rutting

Since the early 1970s, steel reinforcement has been abandoned in the US due to the aforementioned installation difficulties. However, in the early 1980s, interest in the use of this interlayer product for reinforcement applications increased in Europe, especially in Belgium and the Netherlands. The steel mesh that is used today is coated against potential rust, and the installation techniques have been significantly modified. The configuration of the current steel mesh product consists of a double-twist, hexagonal mesh with variable dimensions, which is transversally reinforced at regular intervals with steel wires, either circular or torsioned flat-shaped, inserted in the double twist, as shown in Figures A-1(a) and (b).

(a)

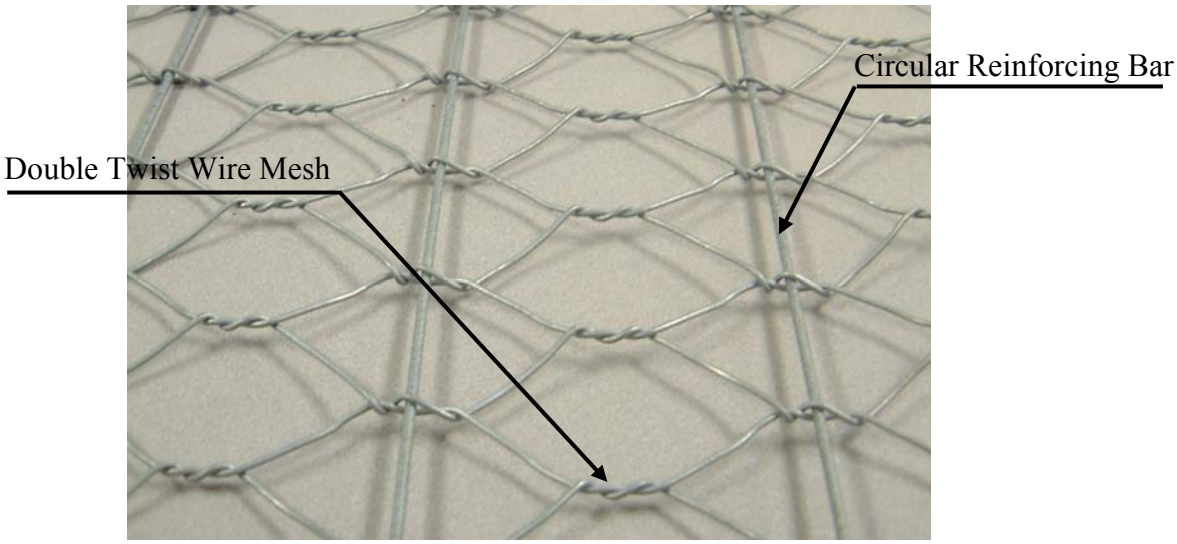

(b)

Figure A-1. General Configuration of Two Types of Steel Reinforcement Nettings

Table A-2 illustrates a general comparison between the original steel mesh and the new product. No welding is used in the new generation of steel reinforcement. This greatly reduces installation difficulties, as well as any variation in HMA densities due to welded reinforced steel.

A.3.3.2 A New Class of Steel Reinforcement

With the growing need for new rehabilitation methodologies to increase the service life of repaired pavements, the new class of steel reinforcement has been mainly evaluated in the reinforcement of HMA and overlays. Steel reinforcement has been installed in several trial sections in Belgium (Belgium Road Research Center [BRCC] 1995). The performance of the test sections was monitored for a service life ranging from two to ten years. The original conditions of each test site, as well as its traffic volume, are illustrated in Table A-3.

Table A-2. Comparison between the Original Steel Mesh and the Current Steel Netting

Criterion	Original Mesh (1950-1970)	New Mesh (1980-2000)
Product	Welded wire	Coated mesh
Product Shape	Rectangular	Hexagonal
Sensitivity to rust	Yes	No
Installation	Rigid	Allows horizontal movement
Unrolling Process	Manually	Using a roller
Creeping of the mesh	Installed loose	Wire tension may be relieved during construction
Fixation	Hog rings	Nails or other pertinent method (slurry seal)
Cost ($/m^2)	0.20-0.70*	3.5-6.0

* Cost as of 1970.

Table A-3. Performance of Ten Different Field Trials

ID	Project	Year	Area (m^2)	Cause of Deterioration	Fixing Technique	Original Pavement Structure	Traffic Pattern	Road Type	Rehabilitation Strategy*	Performance
1	Brugge	1989	2000	Rutting	Nails	Semi-rigid	Heavy	Urban	80mm L + M + 70mm HMA	Good
2	Beervelde	1991	5000	Rutting	Nails	Flexible	Heavy	Highway	M + 100mm HMA	Good
3	Bellegemstraat	1990	17000	Rutting and cracking	Nails	Rigid and Flexible	Medium	Rural	M + 100mm HMA	Very Good
4	Lange Rei	1989	5000	Cracking	Nails	Semi-rigid	Medium	Urban	M + 50mm HMA	Excellent
5	Zwalm	1991	13000	Cracking	Nails	Rigid	Medium	Rural	40mm L + M + 60mm HMA	Excellent
6	Maldegem	1991	13000	Cracking	Slurry Seal	Rigid	Medium	Rural	R + M + S + 40mm HMA	Good
7	Mont-St-Aubert	1989	7200	Cracking	Nails	Rigid	Light	Rural	M + 70mm HMA	Very Good
8	Nijverheidslaan	1992	4500	Cracking	Slurry Seal	Rigid	Light	Industrial	50mm HMA + M + S + 40mm HMA	Excellent
9	Bernem	1991	12000	Cracking	Slurry Seal	Flexible	Light	Rural	60mm L + M + S + 60mm HMA	Very Good
10	Grimbergen	1992	2500	Rutting and Cracking	Slurry Seal	Flexible	Medium	Industrial	S + 50mm HMA + M + S + 50mm HMA	Fair

* L: Leveling Layer – M: Mesh – S: Slurry Seal – R: Local Repair

The results of the monitoring program are also shown in Table A-3. Based on the results of the monitoring program, several specific observations were made:

- In Project 1 (Brugge), up to 200mm of rutting was measured before repair. After five years of service, a maximum of 20mm of rutting was measured in the sections with steel reinforcement, while a maximum of 35mm of rutting was measured in the sections without steel reinforcement. The non-reinforced sections are one year older, but are not located in a stoppage area (away from the red light), while the reinforced sections are located in the stoppage area. The same trend was also observed in Project two.
- Some putholes were formed in three projects (Projects seven, nine, and ten). This was explained by the fact that the steel-reinforcing netting may have been allowed an excessive freedom of movement that may have resulted in a loss of bonding between the interlayer and the overlay.

Five out of eight projects designated to evaluate the effectiveness of steel netting in abating the reflection of cracks performed satisfactorily (excellent to very good conditions). One of the projects (project ten) showed a fair to poor performance due to poor drainage conditions at the site. Based on the observed performance in these different trial sections, Vanelstraete and Francken concluded that steel reinforcement is effective in reducing reflection cracking (Vanelstraete and Francken 2000). In general, the performance of the overlay was enhanced if slab-fracturing techniques were used to reduce vertical movements at the joints prior to placement of the overlay. It was also concluded that overlay thickness still remains the major factor in pavement performance. Among the evaluated test sites was a project in Mont-Saint-Aubert. This site consisted of a highly deteriorated rigid pavement structure with a traffic pattern classified as light to medium; see Figure A-2(a). In 1989, steel reinforcing netting was installed after minor repairs to the existing pavement structure. A 70mm overlay was then applied on top of the steel netting. Figure A-2(b) illustrates the same road after 11 years of service (2000). After ten years of service, inspections of this site showed a reflective cracking occurrence of only one percent.

(a) (b)

Figure A-2. Comparison between a Road in Belgium: Before Repair and Eleven Years After Repair (after Al-Qadi et al. 2002)

Based on the trial sections performance, Veys recommended that crack and seat should be used if the existing concrete pavement is unstable. A minimum overlay thickness of 50mm with a slurry seal, or 60mm without slurry seal, is recommended above the interlayer system (Veys 1996). Veys also discussed the influence of the fixing technique on steel nettings performance. The use of slurry seal offers many advantages, including preventing water from penetrating into the underneath layers, a better bonding between the interlayer and the existing pavement, and facilitating the placement of the top layer. Research at the BRCC also showed that slippage of the overlay is substantially reduced when slurry seal is used. Francken and Vanelstraete reached a similar conclusion based on various field installations of steel reinforcement (Francken and Vanelstraete 1992). Francken and Vanelstraete found that nailing of steel reinforcement is unreliable and may cause delamination in the overlay. It was also observed that any movement of the interlayer during placement and compaction of the overlay becomes uncontrollable and may negatively affect the performance of steel reinforcement.

Veys also discussed the recycling alternatives for steel reinforcing nettings (Veys 1996). The recycling of steel reinforcing netting should be performed in two steps. The first step consists of milling the HMA overlay down to 10mm above the reinforcement. The second step consists of pulling out the reinforcement using a hydraulic crane. Each material should be individually extracted because the steel is of high quality and can be reused.

Makela et al. presented the Finnish experience with steel reinforcement based on the evaluation of ten different sites where steel reinforcement was used to enhance the bearing capacity of the road and prevent pavement damage by frost heave (Makela et al. 1999). It is worth noting that steel reinforcement was sometimes installed at two different locations within the same pavement structure (inside the base layer, and on top of the existing pavement prior to the overlay installation). This test site has been reported to function well for over twelve years without major problems. It should be noted also that the steel mesh product used is not hexagonal in shape, but rectangular. Also the reinforcement was not placed in the transverse direction, but in the longitudinal direction (parallel to the direction of traffic). The authors reported that for all test sites, steel meshes have prevented frost damage, which usually appear as longitudinal cracks in the pavement surface, while the controlled sections have been significantly damaged.

Corrosion of hot dip galvanized wire reinforcement was evaluated based on collected field samples (Bekaert 1989). Asphalt binder reacts neutrally with galvanized steel, but oxidation due to air and UV light can initiate the corrosion process. This process is further accelerated by the presence of moisture within the pavement. The corrosion process may also be prompted if steel reinforcement gets in contact with an emulsifier. To investigate the effects of the corrosion process on steel reinforcement, samples were collected from several locations including field trials in the Netherlands. Some of the samples were collected after twelve years of service.

Based on the results of this study, the loss in zinc was found to mainly take place during the first years, and then start to level out after that. It was also found that the loss in zinc is approximately 54.5 g/m^2 after ten years, and 58.1 g/m^2 after fifteen years. Based on these results, the applied amount of wire coating was found to be sufficient to resist corrosion by oxidized bitumen. However, it is recommended to limit the amount of emulsion used around the interlayer, while being careful to avoid affecting the bond between the interlayer and the surrounding layers.

Brown and his colleagues investigated the effectiveness of different interlayer systems (geogrid, steel reinforcement, and glass fiber) in preventing the reflection of cracks in HMA overlays based on laboratory testing (Brown et al. 2001). A repeated load shear test was first used to evaluate the interface shear strength and stiffness for

unreinforced and reinforced samples. The results of this set of testing indicated that only steel reinforcement provides interface shear stiffness comparable to the unreinforced case. Both geogrid and glass fiber caused a significant reduction in the interface shear stiffness.

A set of four-point bending tests were performed to establish the contribution of reinforcement to the fatigue life of HMA. Beam sample dimensions were 400 x 120 x 200mm. An interface was created in all samples at a height of 30mm, where the reinforcement (if any) was placed. Although the normal procedure would require that an equal vertical load be applied in both directions to minimize the permanent deformation of the beam, it was found that such a procedure would result in the possibility of crack initiation from the top, bypassing the effect of the reinforcement. Therefore, a greater downward load was applied to ensure that the crack would initiate from the bottom of the beam. The results of this test indicated that the contribution of the reinforcement is negligible under these conditions. The presence of the reinforcement was found to have no effect on the initiation of the crack, or on the early stages of crack propagation.

A semi-continuous fatigue test fixture was then utilized to evaluate the fatigue life of 400 x 200 x 90mm thick beam samples. Reinforcement was placed 30mm above the base, and support was provided by two rubber layers placed over a steel base. A parallel set of laboratory tests was also performed to evaluate the effect of interlayer systems on thermally-induced loading due to the expansion and contraction of a concrete base. This fixture simulated an HMA overlay over a jointed concrete. The joint was slowly opened until failure of the specimen occurred.

Based on the results of this study, the authors suggested that steel reinforcement might improve fatigue life by a factor up to three. Glass fiber was less effective, improving fatigue life by a factor of 1.2. It was also found that all interlayers were effective in preventing reflective cracking due to the thermal movement of a concrete slab, particularly geogrid and glass fiber, giving an improvement factor of up to eight.

Veys studied the effectiveness of steel reinforcement in reducing thermally-prompted reflective cracking based on laboratory testing (Veys 1996). Based on the results of this experimental program, Veys concluded that all tested interlayer systems

delayed the appearance of reflective cracking under thermal loading, while steel reinforcement prevented the crack propagation process.

Coni and Bianco investigated the crack propagation process in the presence of steel reinforcement based on a FE model (Coni and Bianco 2000). The developed FE model simulated a pavement structure consisting of a HMA layer (30mm), a base course (40mm), a base layer (100mm), a subbase layer (200mm), and a subgrade soil. An elastoplastic behavior was assumed for all materials (except steel reinforcement, which was assumed linear elastic), and friction was considered at all interfaces. Both static and dynamic analyses (modal and harmonic analyses) were considered in this study.

The results of the static analysis indicated that steel reinforcement causes a reduction in the surface vertical deflection and tensile stress in the reinforced layer. However, steel reinforcement had no influence on vertical stress components. The results of the dynamic analysis showed that steel reinforcement reduces the stress and strain level in the pavement structure, especially when resonance frequency occurs, at which point the stress and strain levels become very high.

Senstad presented Norway's experience with steel reinforcement in bituminous applications, which are regularly used in Norway to prevent pavement damage due to frost heave and to increase pavement structural capacity (Senstad 1994). Senstad showed theoretically that the tensile strength of frozen pavement is far greater than the tensile stress applied by traffic loading. However, when frozen structures start to thaw, their pavement tensile strength is reduced dramatically and can be easily exceeded, which may result in crack initiation and propagation. To compensate for the lack of tensile strength, a stiff interface (steel reinforcement) may be needed to prevent longitudinal cracking of the HMA layer. Based on beam and multi-layer theory, Senstad found that a steel reinforcement interface could reduce the tensile strain in the HMA layer by as much as 17%.

Francken and Vanelstraete presented their understanding of the steel reinforcement contributing mechanism (Francken and Vanelstraete 1992). According to the authors, the crack initiation and propagation process consists of three distinct phases:

- Overlay is not affected by the existing crack in the existing pavement.

- Crack initiation phase.
- Propagation phase.

The authors believe that the main contribution of the interlayer system would appear in phases one and two only, rather than in phase three. Emphasis was therefore placed on the initial condition of the overlay, and to the crack initiation process. A theoretical simulation of a semi-rigid pavement structure was considered based on a two-dimensional finite element model for thermal and traffic loading.

For thermal loading, different cases, which all consisted of an HMA overlay (40, 70, and 120mm) on top of a cracked continuous concrete pavement structure (70mm), were considered. A homogeneous interlayer system was assumed between the HMA overlay and the concrete layer (Stress Absorbing Membrane Interlayer [SAMI, E=20MPa], metallic grid [E=10000MPa], metallic grid over 2mm slurry seal [E=100MPa], metallic grid over 2mm SAMI [E=20MPa]). The results of the analysis indicated that a soft SAMI interlayer or a composite system consisting of a metallic grid over 2mm of SAMI are the most effective methods to combat reflective cracking prompted by thermal loading. A SAMI interlayer was found to reduce the tensile strain in the overlay by a factor of 30, while a metallic grid over 2mm of SAMI was able to reduce the tensile strain in the overlay by a factor of 60. A stiff interlayer was found less effective; it only reduced the strain in the overlay by a factor of 16.

For traffic loading, a typical semi-rigid pavement structure consisting of an HMA overlay (E=10,000MPa), on top of a 70-mm cracked concrete layer (E=30,000MPa), supported by a soft subgrade (E=40MPa) was considered. Full bonding was assumed between the different layers. A homogeneous interlayer system with varying stiffness (SAMI [E=100MPa], woven geotextile or geogrid [E=1000MPa], 2mm of HMA [E=10000MPa], metallic grid [E=15000MPa], and a metallic grid on top of 2mm of slurry seal [E=100MPa]) was simulated between the overlay and the concrete layer. The position of the load (centered load) on top of a centered crack limited the analysis to mode I movement of the crack. The results of the analysis indicated that all interlayer systems were effective in reducing the strain at the bottom of the overlay. For a greater distance above the crack tip (more than 3mm), it was found that only interlayers with

comparable or larger stiffness than the HMA reduced the strains and the crack initiation time. Interlayers that were not as stiff as the HMA caused an increase in the strains compared to pavement structures without interlayers.

Brown et al. also presented a theoretical approach to simulate the semi-continuously supported beam test, the results of which were previously presented in the laboratory evaluation section (Brown et al. 2000). They suggested the following HMA fatigue model, which is similar to the Paris Law that is used in fracture mechanics:

$$\frac{dc}{dN} = A\varepsilon^{n} \tag{A.1}$$

where

c = the crack length;

N = number of load applications;

ε = maximum tensile strain in the HMA; and

A and n = material constants.

The major difference between this approach and the classical fracture mechanics theory is that this approach assumes that no increase in the straining actions (no intensity) would occur in the vicinity of the crack tip due to the singularity. In other words, the presence of the singularity is neglected in the model formulation. Assuming a formulation of the problem as a beam resting on elastic foundations, the maximum tensile strain in the beam was calculated. This model, which was found appropriate to fit the laboratory results and thus form the basis for predictions of pavement performance, was defined as follows (Brown et al. 2000):

$$\varepsilon = \frac{1}{E}\frac{6M}{(h-c)^{2}} \tag{A.2}$$

where

E = stiffness;

M = bending moment;
h = height of the beam; and
c = crack length.

BRCC evaluated the effectiveness of the Bitufor steel reinforcing netting in delaying the reflection of cracks in flexible pavement applications (BRCC 1998). A 3D finite element simulation was performed for a typical flexible pavement structure consisting of a 200mm subbase layer, a 200mm base layer, an 80mm cracked HMA layer, and an HMA overlay (60, 90, 120, and 150mm). A 5mm-wide crack was induced in the existing HMA layer. Steel reinforcing netting was placed between the existing HMA layer and the overlay. An exact simulation of the steel reinforcement was achieved, but was only placed in the vicinity of the crack to reduce the size of the finite element model. Based on the model symmetry, only one quarter was considered. Two sets of boundary conditions were considered. Evaluation of the interlayer systems was based on selected performance criteria (vertical deflections, and shear strains in the overlay).

The results of this analysis indicated that the decrease in deflection due to steel reinforcing netting is relatively small. It was also found that the deflections on the side not subjected to loading are greater when steel reinforcement is used. This conclusion was based upon the fact that the steel netting allows for a better transfer of the load from the loaded area to the unloaded area. The authors clearly outlined the analogy between steel reinforcing netting in flexible pavements and dowel bars in rigid pavements. Based on a defined mean deflection factor under the load, it was found that the overlay thickness savings due to the steel reinforcement is between five and 10%, depending on the original overlay thickness. Based on the shear strain performance criterion, however, it was found that steel-reinforcing netting is very effective in reducing the shear strain at the vicinity of the crack. In comprising the vertical strain on top of the subgrade for the reinforced and non-reinforced sections, the FE models showed that the steel reinforcement contribution is negligible.

BRRC also compared the effectiveness of two interlayer systems, the Bitufor steel reinforcing netting and the Trasyn glass fiber grid, for preventing reflecting cracking under thermal and traffic loading (BRCC 1999). Exact modeling of each interlayer

system was achieved (non-homogeneous layer with openings) using a 3D finite element. The developed model simulated a semi-rigid pavement structure consisting of an HMA overlay (40 and 100mm) on top of a cracked concrete layer. All materials were assumed linear elastic. Thermal loading was simulated by imposing a 0.2mm opening at the bottom of the crack. A preexisting crack was assumed in the concrete layer with a 5mm depth. To calculate the modulus of elasticity of the glass grid, the mixture law was considered. The calculated grid stiffness modulus was 36,400MPa. Evaluation of the interlayer systems was based on selected performance criteria (tensile strain for thermal loading and shear strain at the vicinity of the crack for traffic loading). The gain provided by an interlayer system is calculated with reference to the 100mm non-reinforced HMA overlay as follows:

$$C_r = \frac{N}{N_{ref}} = \left[\frac{\varepsilon_{ref}}{\varepsilon}\right]^{4.76} \quad \text{(A.3)}$$

where

C_r = relative gain factor;

N = crack initiation time in a given pavement structure;

ε = maximum thermal strain in the structure; and

ref = quantities calculated for the reference structure.

The results of this analysis indicated that both steel netting and glass-grid are effective in reducing thermally-induced reflective cracking (the improvement due to glass-grid was 3.2 to 5 times that of a non-reinforced pavement structure depending on the overlay thickness, while for the steel netting, the improvement was 6.4 to 8.8 times). For traffic loading, both interlayer systems were found to be effective in reducing the shear strain in the vicinity of the crack. However, steel reinforcing was more effective than the glass-grid. This was due to the higher elastic modulus and thickness of steel netting compared to the glass-grid.

A.3.4 Asphalt-Rubber Interlayer

A Stress Absorbing Membrane Interlayer (SAMI) is constructed by placing a seal coat made of rubber asphalt binder (80% asphalt cement and 20% ground tire rubber from old tires) on the surface of the old pavement and then rolling in coarse aggregate chips (Barksdale 1991). This layer may be used as a surface treatment (not recommended because of loss of aggregates) or can be covered with a conventional overlay to act as a stress-relief interlayer.

The main role of the SAMI is to retard crack propagation and improve the tensile strength at the bottom of the overlay due to the presence of the rubber asphalt binder (Molenaar et al. 1986). It is thought that this interlayer will cause the overlay to behave independently from the underlying structure. If this hypothesize is correct, higher tensile strains will occur in the overlay, but no reflective cracking will take place. Most of the reviewed literature agreed on the effectiveness of this interlayer to retard reflective cracking. However, Epps et al. suggested that more research and field evaluation is needed before conclusive recommendations can be made (Epps et al. 2000). Moreover, the effectiveness of rubber asphalt binder is not yet clear, since it was found to perform similarly to straight asphalt binder (Barksdale 1991).

A.4 INTERLAYER INSTALLATION

The installation of interlayer systems is the key to good performance. To address the installation difficulties encountered with some interlayer systems, major modifications have been recently suggested (especially with geogrid and steel reinforcement). For any interlayer system installation, five major steps are required.

First, the pavement surface must be prepared for installation. In this step, the existing cracks and joints are treated in preparation for an overlay (by filling larger cracks or joints with a compressible material, and then covering it with a strip of bond breaking material). The treatment of the existing pavement can also involve breaking up a concrete slab into smaller pieces or pulverizing an existing HMA pavement (Roberts et al. 1996). It was found that breaking and seating concrete slabs before applying the

overlay and the interlayer may contribute to a better performance of the interlayer in delaying reflective cracking (Vanelstraete et al. 2000). However, this procedure reduces the overall bearing capacity of the existing pavement, which has to be balanced by a slight increase in the overlay thickness.

The second step is the application of a fixing layer, or tack coat. The fixing layer ensures strong bonding between the supporting layer and the interlayer system. Applying the correct amount of tack coat ensures good bonding between the existing pavement and the interlayer, and prevents slippage at the interface, which is essential for adequate performance of the interlayer (Button 1989). Application of an insufficient amount of tack coat results in poor bonding between the interlayer and the surrounding material, while application of an excessive amount of tack coat results in slippage problems. Different methods have been suggested for determining the optimum tack coat content (California melt-through test, Texas asphalt retention-shrinkage test, etc.). Smith proposed the following empirical equation to determine the optimum tack coat rate (Smith 1983):

$$RTC = 0.05\ (TW)^{0.30} \tag{A.4}$$

where

RTC = recommended tack coat rate (gal/yd^2);

T = fabric thickness (mils); and

W = fabric weight (oz/yd^2).

The third step is the installation of the interlayer product. This step involves unrolling the interlayer product, as well as any fixation steps (e.g. nailing, tensioning) required after installation. For a better interlayer performance, the interlayer should be laid perfectly flat and any wrinkles or folds should be avoided. For a galvanized steel netting, a loader can be driven over the interlayer to remove any existing tensions and to help flatten the mesh with the existing surface. Steel nails are used to hook the single wire mesh (neither the double twist nor the reinforcing bars of the mesh have to be fixed). For a geogrid, a loader is not used to flatten the interlayer, as it may damage the product. In this case, one

end has to be nailed and the other end stretched using special equipment (pre-tensioning). The pre-tensioning of the geogrid also contributes to the elimination of grid shrinkage during paving. Additional nails are then placed to fasten the grid to the pavement. Because of the problems often encountered in the grid installation, manufacturers recommend the use of a nonwoven fabric attached to the grid resulting in a geocomposite product. Figure A-3 illustrates the unrolling process of a geotextile after application of a tack coat.

Figure A-3. Unrolling Process of a Geotextile after Application of a Tack Coat

The fourth step is the application of an intermediate layer. This layer is used for protection, or for providing a waterproofing benefit to the interlayer. In the geogrid installation, a surface dressing, such as a chip or slurry seal, is usually applied to protect the interlayer from any damage or buckling that may occur during paving. In the steel mesh installation, a slurry seal is also recommended to provide a strong bonding to the existing pavement, reduce water infiltration to the underneath layers, and provide extra-elasticity to the interlayer system (Veys 1996). Figure A-4 illustrates the application of a slurry seal on top of a steel reinforcement interlayer.

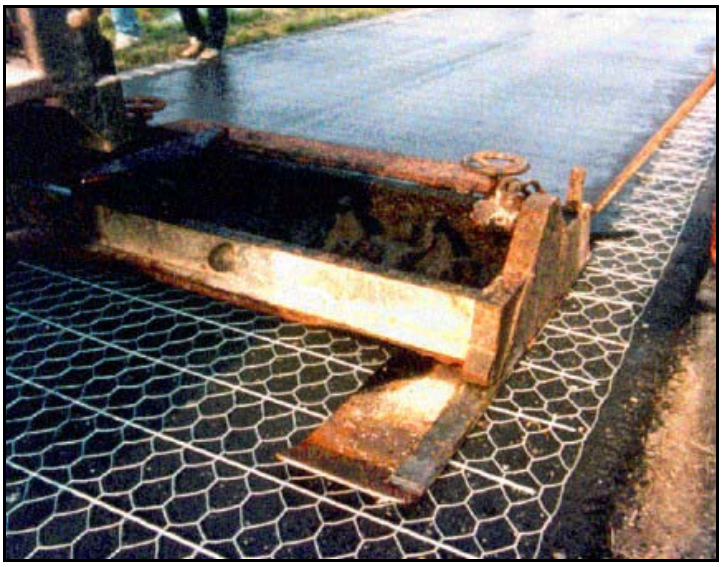

Figure A-4. Application of a Slurry Seal on Top of a Steel Mesh Interlayer

The fifth step is the application of an upper layer or HMA overlay. This step consists of applying the upper layer to the interlayer system (HMA or granular layer). All previous steps dictate how successful the paving operation will be. The major problems faced during application of the upper layer are buckling of the interlayer, shrinkage of the plastic product (if heat sensitive), and poor density of the compacted layer. Most of these problems may be avoided by good fixation and protection of the interlayer. Figure A-5 presents a summary of the interlayer installation.

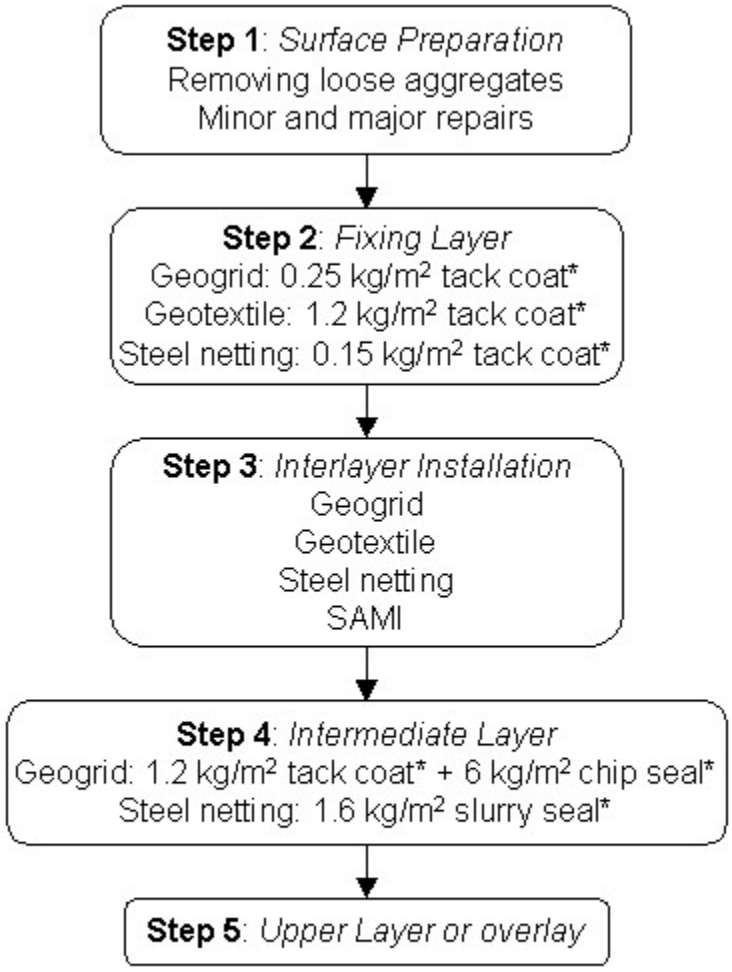

Figure A-5. Installation Procedure for an Interlayer System

A.5 DESIGN OF FLEXIBLE PAVEMENTS WITH INTERLAYER SYSTEMS

Very little is known about the exact method that one uses to design a pavement system incorporating an interlayer system. Until now, most of the design methods presented to account for interlayer contributions to a pavement system have depended upon the fact that an interlayer should result in a reduction of the required layer thicknesses to reach the same level of performance, and to be cost-effective at the same time. However, this can only be true if the interface system is reinforcing a pavement system. Another

problem lies in the fact that most of the interlayer contributions are not yet quantifiable. The following section provides a quick overview of some of the developed "design" methods that are used to account for interlayer contributions.

A.5.1 Moisture Barrier Interlayer

If an interlayer is providing a waterproofing benefit to the pavement system, the main modification to the conventional design is an improvement in the drainage coefficients used to calculate the pavement structural number (SN), based on the AASHTO design method (AASHTO 1986):

$$SN = a_1D_1 + a_2D_2m_2 + a_3D_3m_3 + \ldots..+ a_nD_nm_n \quad (A.5)$$

where

a_1, a_2, a_3, … a_n = the layer coefficients;

D_1, D_2, D_3, … D_n = the layer thicknesses; and

m_2, m_3, …. m_n = the drainage coefficients.

The drainage coefficients should range between 1.4 to 1.2 for excellent drainage conditions and 0.95 to 0.40 for poor drainage conditions (Marienfeld et al. 1999). The quality of drainage is measured by the length of time for water to be removed from the pavement (Huang 1993). Since the determination of drainage coefficients is mainly based on engineering judgment and previous experiences, the advantage given for using an effective waterproofing interlayer or the penalty charged for a poor drainage system is not well-defined.

A.5.2 Separation Interlayer

When functioning as a separation layer, an interlayer prevents the intrusion of fines from the subgrade into the base layer. To account for this contribution, Bhutta suggested the assumption that a transition layer would occur if a separation geotextile was not used at

the subgrade level (Bhutta 1998). This transition layer would have a resilient modulus between the base and the subgrade moduli due to the expected mixing between the upper layer (base or subbase) and the subgrade fine particles. To determine the thickness and resilience modulus of the transition layer, an iterative process based on backcalculation was suggested. It is clear that this problem does not have a unique solution. Moreover, Bhutta claimed that the transition thickness is not constant, but sharply increases with time until it reaches an asymptotic level. Although the suggested hypothesis seems realistic, a parametric study is essential to identify the variation of this transition layer with the different design parameters, including subgrade type, percentage of fines in the subgrade, and base type.

A.5.3 Reinforcing Interlayer

It was previously shown that in order to act as reinforcement, an interlayer must have a stiffness higher than that of the surrounding materials. In this case, the interlayer may provide a substantial savings in the overlay thickness, and the proposed design method should reflect this concept. Based on laboratory testing, Lytton defined a reinforcing mode that presumes that debonding must occur between the interlayer and the existing pavement before failure can take place (Lytton 1989). The suggested equation for overlay design incorporating a solid interlayer takes the following form:

$$d_0 = \frac{k_0 \Delta}{(f_{t0})\beta \sinh(\frac{\beta w}{2})}\left[\cosh\frac{\beta w}{2} - 1\right] - nt_f \qquad (A.6)$$

where

d_0 = the required thickness of the overlay;

k_0 = the shear stiffness of the tack coat;

$\beta = \sqrt{\frac{k_0}{E_u d_u}}$

E_u = the elastic stiffness of the under-layers; and

d_u = the combined thickness of the existing pavement.

f_{t0} = the design tensile strength of the overlay;

w = the minimum width of the interlayer placed above the existing pavement;

n = the elastic stiffness ratio (ratio of the elastic stiffness of the interlayer to the elastic stiffness of the overlay;

t_f = the thickness of the interlayer; and

Δ = the crack full width opening.

A similar equation was provided for an interlayer system with openings:

$$d_0 = \frac{k_0 \Delta}{(f_{t0})(1+np)\beta \sinh(\frac{\beta w}{2})}\left[\cosh\frac{\beta w}{2} - 1\right] \quad \text{(A.7)}$$

where

all of the repeated variables are defined as before; and

p = the ratio (in decimal form) of the cross-sectional area of the interlayer divided by the cross-sectional area of the overlay.

Vanelstraete et al. proposed another design method based on 3D finite element simulation. Vanelstraete et al. suggested the use of design charts to evaluate the substantial saving in overlay thickness when steel reinforcement is used on top of rigid pavement (Vanelstraete et al. 2000). Shear strain at the bottom of the overlay (mainly responsible for slab rocking) and surface deflection were used as bases of comparison. The followed approach seems promising, since the finite element method is a complex and costly analysis tool that cannot be used in routine design. However, for successful implementation, the finite element model should first be calibrated based on experimental measurements, and a parametric study should then be performed using the calibrated models to evaluate the effects of the different design parameters.

A mechanistic design procedure for geosynthetic reinforced flexible pavement was proposed by Majidzadeh (Majidzadeh et al. 1982). This design method is based on

the two traditional failure modes considered in any mechanistic design method: fatigue of the HMA and rutting of the subgrade. The rutting of the subgrade is assumed to be directly caused by the vertical strain at the top of the subgrade layer; the HMA fatigue is caused by the horizontal tensile strain at the bottom of the HMA layer. The relationship between the critical strain at the bottom of the HMA and the number of cycles for fatigue failure is expressed as follows:

$$N_f = c_1\left(\frac{1}{\varepsilon_h}\right)^{m_1} \text{ for controlled stress tests} \quad (A.8)$$

$$N_f = c_2\left(\frac{1}{\varepsilon_h}\right)^{m_2} \text{ for controlled strain tests} \quad (A.9)$$

where

N_f = fatigue life of a flexible pavement;

ε_h = maximum tensile strain or tensile stress; and

c_1, c_2, m_1, and m_2 = parameters determined by laboratory beam testing.

To consider the contribution of the interlayer, Majidzadeh et al. introduced the following parameter:

$$\text{FEF} = \text{Fabric Effectiveness Factor} = \frac{N_{fr}}{N_{fu}} \quad (A.10)$$

where

N_{fu} = unreinforced number of fatigue cycles (determined from equation A.8 or A.9);

N_{fr} = reinforced number of fatigue cycles determined as follows:

$$N_{fr} = N_{fu} \times \text{FEF}(i, \varepsilon_h) \times \text{GEO} \quad (A.11)$$

where

$\text{FEF}(i,\varepsilon_h)$ = value of FEF for fabric i at strain h; and

GEO = geometry correction effected by the depth of fabric in the HMA layer.

To determine, the Fabric Effectiveness Factor (FEF) in Equation (A.11), Majidzadeh suggested the following equation:

$$FEF = a_1(\varepsilon_h)^{a_2} \quad (A.12)$$

where

a_1 and a_2 = parameters to be determined from laboratory testing of beams reinforced with geosynthetics.

GEO is related to the depth of interlayer from the top of flexible pavement (d'), the depth of the neutral axis (zero horizontal bending strain, (z) under the traffic load). GEO is limited to the value of 1.0, and is determined as follows:

$$GEO = 0.64\ (d'/z)^{1.60} \quad (A.13)$$

It may be noticed that this method required excessive testing to evaluate the contribution of the interlayer, which may not be ideal for use in routine design. Moreover, the flexibility to select different mode of failures based on each case, which was offered in the previous method, is not available in this method, which only considers the fatigue failure mode. Moreover, thermal loading is not considered in this method.

The last design method presented here was suggested by Kennepohl for the design of flexible pavements incorporating a geogrid interlayer as base reinforcement (Kennepohl et al. 1985). Recalling Equation (A.5) that is used to calculate the structural number (SN) based on the 1986 AASHTO design guide:

$$SN = a_1D_1 + a_2D_2m_2 + a_3D_3m_3 + \ldots..+ a_nD_nm_n \quad (A.14)$$

Kennepohl et al. suggested the modification of this equation to account for the geogrid benefits as follows:

$$SN = a_1D_1 + \alpha a_2D_2m_2 + a_3D_3m_3 + \ldots.. + a_nD_nm_n \quad (A.15)$$

where

α = a layer coefficient ratio representing the reinforcement effect of the geogrid. This coefficient is determined based on laboratory testing (circular plate loading test) as follows:

$$\alpha = \frac{a_r}{a_u} = \frac{SN_r \, x d_u}{SN_u \, x d_r} \quad (A.16)$$

where

a_r and a_u = layer coefficients for the reinforced and unreinforced case;

SN_r and SN_u = structural numbers of the reinforced and unreinforced sections (determined from the AASHTO design monograph, knowing the subgrade soil support value, the number of load repetitions to failure for each test, and the pavement thickness); and

d_u and d_r = layer thickness (reinforced and unreinforced).

Kennepohl et al. presented different examples of how to determine the layer coefficient ratio, and indicated that this coefficient may be estimated for all design situations. This method seems promising, since it can be easily incorporated in the usual AASHTO design method. However, prior to full validation, establishing an appropriate link between the plate loading test, and actual traffic loading is essential so interlayer contributions can be accurately considered.

A.5.4 Stress Relieving Interlayer

When an interlayer system is acting as a stress-relieving layer, a dissipation of energy is anticipated that is otherwise part of the crack propagation process. It was previously emphasized that a stress-relief interlayer does not justify a reduction in the overlay thickness since it does not contribute to the structural capacity of the pavement system.

The main contribution expected from a stress-relief layer is a retardation of crack reflection. Therefore, a fracture mechanic approach is necessary to understand the crack propagation process. Different studies have used this approach through the common empirical power law developed by Paris and Erdogan (Paris and Erdogan 1963):

$$\frac{dc}{dN} = A(\Delta K)^n \tag{A.17}$$

where

c = crack length;

N = number of loading cycles;

A and n = fracture parameters of the material; and

ΔK = stress intensity factor amplitude.

The stress intensity factor K is depending on the considered geometry, and the mode of crack propagation (Owusu-Antwi et al. 1998):

- Mode I loading results from loads that are normally applied to the crack plane.
- Mode II loading results from in-plane shear loading, which leads to crack faces sliding against each other.
- Mode III loading results from out-of-plane shear loading, which is negligible for the considered problem.

As an acceptable approximation, it was found that, although traffic loading contributes to both modes I and II crack propagation processes, the stress intensity factor resulting from mode I (K_{IC}) is negligible compared to the stress intensity factor resulting from mode II (K_{IIC}) (Owusu-Antwi et al. 1998). On the other hand, thermal loading mainly contributes to the mode I crack propagation process. If both types of loading are assumed to occur simultaneously, which will be the critical loading case; the combined stress intensity factor can be calculated as follows (Richard et al. 1983):

$$K_v = 0.5\,(K_I + \sqrt{K_I^{\,2} + (2\alpha_1 K_{II})^2}) \tag{A.18}$$

where

$$\alpha_1 = \left(\frac{2(1-\nu)-\nu^2}{3(1-2\nu)}\right)^{3/2} \tag{A.19}$$

where

ν = the Poisson's ratio of the overlay material.

The number of cycles needed for a crack to grow from length c_1 to length c_2 ($c_2 > c_1$) can be obtained from Equation (A.17) by integration:

$$N = \frac{1}{A}\int_{c_1}^{c_2} \frac{dc}{(\Delta K)^n} \tag{A.20}$$

The main problem associated with the integration in Equation (A.20) is the determination of the stress intensity factor for the considered geometry and loading. Only a limited number of exact solutions exist when the size of the crack is small compared to the dimensions of the body and for very simple geometry (Kanninen et al. 1985).

To overcome this problem, different approximations have been proposed; most are based on the application of the finite element method, which allows for a direct calculation of the stress intensity factor with only minor change to a standard finite element code. Among the different approximations recently proposed, the one suggested by Graf is presented (Graf et al. 1993). To determine the stress intensity factor in mode I loading (due to thermal stresses), Graf made use of the following approximation assuming an uncoupled overlay (unbounded to the existing pavement):

$$K_I\big|_{\gamma_1=0} \cong \sigma\sqrt{\pi c}\; f(\frac{c}{h_1}); \quad 0 \le \frac{c}{h_1} \le 0.5 \tag{A.21}$$

where

K_I = the stress intensity factor due to thermal loading;

γ_1 = a coupling factor, where γ_1=1 indicates full bonding between the overlay and the existing pavement and γ_1=0 indicates an unbounded case;

h_1 = the overlay thickness;

$$f(\frac{c}{h_1}) = 0.265(1-\frac{c}{h_1})^4 + \frac{0.857 + 0.265\frac{c}{h_1}}{(1-\frac{c}{h_1})^{3/2}} \quad \text{(A.22)}$$

and;

$$\frac{\sigma}{\sigma_r} = F_R\left(\frac{c}{h_1}\right) \quad \text{(A.23)}$$

where

σ_r = the thermal surface stress; and

F_R = a function determined with the help of FE calculations.

Another solution was given to determine the stress intensity for mode II loading (traffic loading):

$$K_{II}\big|_{\gamma_1=0} \cong 0.65\frac{Q}{h_1 - c}\sqrt{\pi c}; \quad c < h_1 \quad \text{(A.24)}$$

$$K_{II}\big|_{\gamma_1=1} \cong 2.31\frac{Q}{\sqrt{\pi(h_1 - c)}}; \quad c < h_1 \quad \text{(A.25)}$$

where

Q = the applied shear force.

After defining the stress intensity factor, Equation (A.20) is used to determine the number of cycles before the crack propagates to a specific length c_2 (usually taken as half the overlay thickness, $c_2 = 0.5h_1$). The number of cycles can then be evaluated for different

situations (incorporating a stress relieving layer or without interlayer), and the contribution of the interlayer in delaying the crack propagation process can be evaluated.

Another issue to be faced when using Equation (A.20) is the correct values of the material fracture parameters (A and n). The correct way to determine the fracture properties of a material (A and n) is to examine the stable crack growth of HMA beam samples under repeated loading conditions, which is a tedious and expensive operation (Francken 1993). To overcome this problem, Schapery presented theoretical relations between the fracture properties of a material and its creep, tensile and fracture energy properties (Schapery 1982). These relations were based on both linear viscoelastic theory and the path independent J-integral. For both traffic and thermal loading, the fracture properties of a material can be determined as follows:

$$n = \frac{2}{m} \tag{A.26}$$

where

m = the slope of the log creep compliance versus log time curve. In most cases for typical HMA mixes, the exponent lies between 2.1 and 6.0 (Jayawickrama et al. 1987).

Schapery also showed that for traffic fatigue, and conventional HMA mixes:

$$n = -2.2 - 0.5(\log A_F) \tag{A.27}$$

and for thermal fatigue:

$$n = -0.72 - 0.42(\log A_T) \tag{A.28}$$

A.5.5 Closure

Whether or not an interlayer system positively contributes to a pavement system is largely dependent on its performance in real pavement structures. Prior to implementation, an interlayer system should be fully evaluated in all anticipated

conditions. This evaluation cannot be solely based on laboratory testing, but should include several field evaluations. Moreover, new interlayer products are regularly introduced to the transportation agencies for pavement applications. These new products lack the fundamental supportive information that allows an accurate determination of their benefits to pavement systems. As part of his excellent overview of the subject, Steen summarized the actual interlayer market as follows (Steen 2000):

"Over the years, I have noted many attempts to enter this huge road maintenance market. Every manufacturer within the geosynthetic field seems to have tried to use some of their standard geotextile products as a solution to retard reflective cracking. More or less successfully, however. Each time, expensive, complicated, and overestimated solutions are used in road maintenance, it simply destroys the whole idea of geosynthetic interlayers, and this also reflects on suitable solution."

A.6 INSTRUMENTATION OF FLEXIBLE PAVEMENTS

Due to the difficulty of measurements and the very high cost of road test facilities, very little is known about the actual effects of interlayer systems on pavement structures subjected to dynamic loading. Although it is the only feasible way to develop a fundamental understanding of how interlayer systems can contribute to flexible pavement performance, very few attempts have been made to date on the instrumentation of a flexible pavement incorporating interlayer systems. Prior to presenting the most notable investigations in flexible pavement instrumentation, a general overview of the subject is presented.

Several benefits may result from the instrumentation of pavement systems. First, pavement instrumentation allows the validation of analytical models as well as the calibration of model response variables based on actual data (White 1989). Second, pavement instrumentation helps researchers to develop a better understanding of pavement responses, which is essential if adequate design routines are to be suggested. Finally, pavement instrumentation contributes to the understanding of the effects of

different control variables, such as temperature, moisture, and tire configurations, which are usually not incorporated in current design methods.

When instrumenting a pavement system, pavement response parameters such as vertical stress, horizontal and vertical strains, and deflections are of primary interest. However, environmental parameters such as temperature, frost depth, and moisture content are essential if pavement response data are to be fully understood. For a successful instrumentation strategy, at least two types of response (stress, strain or deflection) should be compared simultaneously (Ullidtz 1987). There are two major categories of testing facility, which aim to better understand pavement performance either by "in-service performance monitoring" or by pavement response instrumentation (Metcalf 1996):

1. Full-scale accelerated pavement testing (APT) consists of "the controlled application of a prototype wheel loading, to a prototype or actual, layered, structural pavement system to determine pavement response and performance under a controlled, accelerated, accumulation of damage in a compressed time period" (Metcalf 1996). This type of facility is usually divided into two main groups:

    - Test road facilities that consist of actual pavement systems, which are used for in-service performance monitoring. The acceleration of damage is achieved by means of increased repetitions (actual truck loading), and modified loading conditions. The main advantage of this type of facilities is the almost 'exact' simulation of actual pavement performance. The main disadvantage is the high initial cost of such a facility ($15,000,000). Although performance can be easily monitored through percentage of cracking and rutting, the exact mechanism of failure is rarely understood. The Wes Track Pavement facility at Nevada is an example of test roads recently constructed (1995). The primary purpose of this test road was the evaluation of the performance of different HMA mixes.
    - Test track facilities where simulated loading is applied by means of loaded wheels or plates to a section of test pavement. There are three basic types of test track, those in which the load is applied through a wheel rotating in a circular track,

those in which the wheel moves in a straight track, and those in which a wheel assembly is constrained to move around a circular or oval pavement section (Metcalf 1996). The main advantage of this type of facilities is the relatively low cost (from $500,000 to $1,000,000) and the fully controlled loading conditions.

2. Full-scale instrumented test facilities consist of "a stretch of highway built or selected for the purpose of observing behavior and performance under controlled special traffic" (Metcalf 1996). To better understand pavement response, extensive instrumentation is required. Soil pressure cells and strain gauges are usually a must in this type of test facilities. Other sensors such as thermocouple, resistivity probe, multi-depth deflectometer, are also regularly used. The Minnesota MnRoad is an example of recently constructed, full-scale instrumented test facilities (1993). More than 4500 different sensors were used in this project to evaluate different HMA, concrete, and gravel sections. The main advantage of such facilities is their ability to contribute to the current state of knowledge in pavement engineering through a better understanding of pavement response and performance. The main disadvantages are the initial high cost of such facilities (around $25,000,000) and the tremendous amount of data to be analyzed, which requires an efficient routine if it is to be effectively managed and organized.

A.6.1 Pavement Sensors

Since their introduction in the early 1900s, pavement sensors have evolved and are now capable of providing accurate and reliable measurements if properly installed and calibrated. Different types of sensors are now available to measure strain, stress, deflection, temperature, frost depth, moisture, etc. It might appear that sensor selection is an easy task, of no great consequence to the data analyst, but quite the opposite is true. Each sensor type has its own advantages and disadvantages, which have to be fully understood prior to the selection of a suitable sensor (Tabatabaee et al. 1990). When selecting a gauge, a compromise has to be reached based on the different decision criteria

involved in the selection. Generally, the decision criteria can be summarized as follows (Measurements Group Inc. 1994):

- The required sensor accuracy
- The stability and reliability of the sensor
- The temperature resistance of the sensor
- The cyclic endurance of the sensor
- The base of installation and survivability expectation
- The range of the sensor readings and its agreement with the required range
- The stiffness of the sensor and its suitability for the working environment
- The calibration requirement for the sensor

If each decision criterion is carefully studied, the selected gauge should be the optimum for the required job. The following sections provide a review of each sensor type**,** along with its advantages and disadvantages.

A.6.1.1 Strain Gauges

To measure strain in flexible pavements, two types of sensors are usually used, depending on the measurement location (Tabatabaee 1990). If measurements are made in bounded layers, electrical resistance strain gauges are used; if measurements are conducted in unbounded (granular) layers, linear variable differential transformers (LVDTs) and special strain gauges (e.g. vibrating wire strain gauge) are used. The most important property of a strain gauge is its stiffness and its variation with temperature (Huhtala et al. 1993). The ideal strain gauge would be one with stiffness equal to the stiffness of the surrounding material at all temperatures. In this case, the measured strain will be the true strain in the material. However, since this is never the case, the selected strain gauge should be as close as possible to the ideal case. If the stiffness of the gauge is much higher than that of the surrounding material, the sensor will act as reinforcement to the pavement system, and the recorded strain will be much lower than the actual strain in the material.

Measuring strains in granular materials is a tedious operation due to their low stiffness, which requires a "soft" gauge that can deform like the surrounding material, but to be able to survive the tough construction practices at the same time. To overcome this problem, strain in granular material is usually accomplished by measuring the differential displacement between two points using LVDTs (Ullidtz 1987).

Static strain measurement, using vibrating wire strain gauges, is also feasible. This gauge, which is primarily designed for long-term strain measurements in mass concrete, can be used for long term monitoring of the strain in granular materials. The advantage of this type of gauge is the use of frequency, rather than voltage, as the output signal from the gauge. Frequency may be transmitted over long cable lengths without significant degradation caused by the cable resistance. Vibrating wire gauges also have excellent long-term zero stability. The installation of this type of gauge is straight-forward and among the easiest of all gauges. The main disadvantage of this type of gauge is that the obtained readings, being static in nature (i.e. not really sensitive to dynamic loading), can only be used for long term monitoring of pavement performance.

Electrical resistance strain gauges have also been tested, but have not been very successful (Ullidtz 1987). The gauge was either too soft to survive the very high loading during construction and compaction of the layer or too stiff to deform after construction due to the low stresses generated in the granular layers.

Deformations in bituminous layers are usually measured using electrical resistance strain gauges. This gauge theory of operation is based on the fact that when a thin wire is stretched, its electrical resistance changes. This change in resistance ($\Delta R/R_0$) can be directly correlated to the mechanical elongation ($\Delta L/L_0$) through a gauge factor based on the following equation (Huhtala et al. 1993):

$$\frac{\Delta R}{R_0} = K\frac{\Delta L}{L_0} \tag{A.29}$$

where

K = the gauge factor.

The major problem with this type of gauge is its durability. If the high strains that the gauge is subjected to during construction exceed its range of operation, it will be damaged or completely destroyed. Therefore, major improvements have been introduced to increase the fatigue and moisture resistance of these gauges. The most common types of electrical resistance strain gauge used in bituminous materials are the Kyowa strain gauge, the Dynatest® H-type strain gauge (also called H-type strain gauge), and the foil strain gauge.

The Kyowa strain gauges were the first H-type gauge to be developed. These gauges consist of a wire of a given material, into which the strain gauge is connected. The ends of the wire are connected to rectangular anchor bars, thus forming the letter H. The main disadvantage of this gauge is its very poor durability. A loss of 30 to 50 percent of the installed Kyowa strain gauges during construction is not unusual (Ullidtz 1987). In previous experiments in the Danish Road Testing Machine (RTM), none of the installed Kyowa strain gauges lasted for the entire experiment (Ullidtz 1989).

H-type strain gauges were recently developed by the Technical University of Denmark to address the poor durability of the Kyowa strain gauges. Unlike the Kyowa strain gauge, this gauge features 27 different layers to protect the resistance wire. The strain gauge is completely embedded in a strip of fiberglass-reinforced epoxy with low stiffness to increase the gauge flexibility. The whole gauge is covered by a bituminous coating to approach the temperature behavior of HMA mixes. The main advantage of this gauge is its outstanding durability compared to the Kyowa gauge. This type of gauge has been used for two years in an unfriendly moisture environment, and has been subjected to more than one million repetitions, without any damage (Ullidtz 1987). The main disadvantage of the H-type strain gauge is its very high cost, as it is manually manufactured.

Foil strain gauges consist of a gauge that is glued to HMA cores (laboratory made or field extracted). The entire item is then installed in the pavement system. The main advantage of this gauge is its very high durability and its flexibility of adjustment in any direction. The major disadvantage is the uncertainty about effectiveness of its bonding between the instrumented core and the surrounding pavement.

Two distinct methods are currently used in strain gauge installation. The choice of method mainly depends on the type of gauge to be installed. No unanimity exists on how to install the gauge with minimum disturbance to the pavement system and with less damage to the gauge itself; engineering judgment is required.

The first method (supported by the Finnish) is mainly used for foil-type strain gauges. This method consists of gluing the gauge to a laboratory-made core sample, which is then installed as part of the HMA layer with a tolerance of less than 1 mm. In this case, the gauge reduces the strengthening effect of the instrument (Huhtala et al. 1991). The main advantage of this method is that the installed gauge does not have an elastic part, which makes it possible to follow the relaxation process of a viscoelastic material as asphalt binder. If damaged, the gauge can be easily replaced. The main disadvantage of this method is the tediousness of installation. Also, it is possible that the coring process might affect the boundary conditions around the gauge; furthermore, it is possible that effective bonding may not be achieved.

The second method is used for all other types of strain gauges. This method consists of installing the strain gauge during layer construction as part of the pavement system. The strain gauge is usually covered by hand-laid bituminous material to create a protective layer. The gauge is then compacted as part of the pavement system. The main advantage of this method is its simplicity. The main disadvantage is that damage to the gauge often occurs due to the high stress applied during compaction (A loss of fifteen percent or less is considered a success). Also, the materials that surround the gauge are usually highly disturbed (being hand laid and if static compaction is used in the instrumented area).

The responses of strain gauges installed in bounded materials are very valuable to pavement engineers. Their dynamic responses help engineers to gain a better understanding of different control variables, such as vehicle speed, tire pressure, temperature, and so forth. During the last two decades, the qualitative analysis of strain signals in the transverse and longitudinal directions have significantly contributed to the current state of knowledge in pavement engineering (Vogelzang et al. 1991). Moreover, if quantitative analysis becomes more feasible, the verification of response and performance models would be possible through effective instrumentation.

A.6.1.2 Pressure Cell Gauges

Earth pressure cells (also called soil stress gauges) consist of a pressure sensor with a transducer to convert the pressure into a measurable signal (Selig 1989). The most common type of pressure cells is the diaphragm cell. The principle of these transducers is that a pressure acting on the diaphragm of the cell will cause a deflection that can be transformed into an electrical signal by strain gauges attached to the inside of the diaphragm (Ullidtz 1989). This type of pressure cell has been proven to give a linear response to the applied stress, regardless of the surrounding stiffness.

Two factors affect pressure cell performance: the ratio of the gauge thickness to diameter (T/D) and the ratio of the gauge stiffness to that of the surrounding material (E_g/E_s). Askegaard has shown, the theoretical signal from a liquid filled pressure cell can be expressed as follows (Ullidtz 1998):

$$q = C\sigma_z + D\,(\sigma_x + \sigma_y) \tag{A.30}$$

where

q = the recorded stress by the cell;

σ_z = the corrected vertical stress;

σ_x and σ_y = the stresses in the plane of the cell; and

C and D = constants depending on the thickness to diameter ratio (T/D) called aspect ratio, and the ratio of stiffness (E_g/E_s).

Ullidtz found that the recorded and correct stresses will be close ($q = \sigma_z$) if the aspect ratio is very small and (E_g/E_s) very high, which means that the cell should be very stiff compared to the surrounding material (Ullidtz 1998). Based on a theoretical analysis, Torry et al. suggested the use of a flexibility factor to evaluate the pressure cell accuracy (Torry et al. 1967). The flexibility factor is defined as follows:

$$\text{Flexibility Factor} = \frac{E_s d^3}{E_c t^3} \tag{A.31}$$

where

E_s = the soil elastic modulus;

E_c = the cell elastic modulus;

d = the diameter of the cell diaphragm; and

t = the thickness of the cell diaphragm.

Based on Torry et al. (1967), the errors in cell measurement will be negligible if the aspect ratio is less than 0.2, and the flexibility factor less than 1.0. Pressure cell installation is the key to good gauge performance. Three different methods can be used, depending on the type of surrounding materials (Selig 1989):

- Excavating and re-compacting the soil (mostly appropriate with soft soil and fine sand).
- Excavating the soil and backfilling with a sand bedding (mostly appropriate with stiffer soil and granular materials).
- Excavating the soil and backfilling with grout (mostly suitable with very hard soil).

The accuracy of pressure cells is not well documented, and a large variability exists among different investigators. The expected accuracy with liquid-filled diaphragm pressure cells is around 25% or less (Selig 1989).

A.6.1.3 Strain Gauges and Pressure Cells Calibration

Three approaches are generally considered when dealing with the subject of sensors calibration. The first approach considers that the gauge factor provided by the manufacturer is far more accurate than the calibration factor obtained by a workshop calibration (Krarup 1992). Therefore, no efforts should be made to recalibrate the instruments, since they will always result in lower accuracy.

The second approach is the opposite of the previous approach. Mechanical calibration is performed to validate manufacturer calibration. The agreement between the

two-calibration methods results in a higher confidence level on the gauge performance. It also increases understanding of the gauge operating mechanism and limitations.

The third approach assumes that, regardless of the accuracy of the manufacturer's calibration, the suggested gauge factor is affected by the followed installation procedure and the homogeneity of the surrounding materials (Huhtala et al. 1997). To address this problem, the technical research center of Finland has suggested the field calibration of sensors after complete installation of the instrument. Two approaches were proposed (Huhtala et al. 1997):

- Calibration of the instruments (strain gauge and pressure cell) using a Falling Weight Deflectometer (FWD). Experiences with this calibration procedure were not successful due to the applied stress distribution under a rigid plate such as that of the FWD loading system.
- Calibration of the instruments (strain gauge and pressure cell) using actual truck loading. In this case, a slow moving truck (5km/hr) passed over the instrument to be calibrated. The gauge factor was then calculated for different thickness of HMA, and the average of all tests was used. If the standard deviation of the gauge factors was within 15%, the instrument was considered in later analysis. If this was not the case, the gauge installation was assumed invalid, even if the gauge response was perfect. The invalid installation was explained by different factors, including high disturbance of the surrounding materials, problems with the gauge itself, and heterogeneity of the laid materials around the gauge.

A.6.1.4 Time Domain Reflectomery

One of the most popular methods for continually measuring the moisture content of pavement systems is time-domain reflectometry (TDR). In this process, a sensor transmits electromagnetic waves along a set of metallic conducting rods. The velocity of the pulse is influenced by the dielectric constant (ε) of the host material. This voltage pulse travels along the waveguide until areas of differing electrical impedance values are encountered. As TDR responses are based on the dielectric properties of the host

material, the measurements can be related to soil moisture content (the dielectric constant of dry aggregates ranges from four to eight; depending on the mineral compositions and the dielectric constant of wet aggregates, it can reach up to 20). This conversion can rely on equations provided by the manufacturer (with an accuracy of ± 2%). However, greater accuracy can be achieved by developing calibration equations from comparisons between moisture contents using the TDR and gravimetric methods (oven drying).

Installation of a time domain deflectometer (TDR) is accomplished by preparing a hole to accommodate the probe in a horizontal position. If large aggregates are present around the probe, they should be removed and replaced by sand (clay or silt-like materials should be avoided). After placement of the gauge, the soil should be compacted carefully around and over the probe.

A.6.1.5 Resistivity Probe

A widely used method for determining frost depth in a pavement structure relies on measuring temperatures. This method considers that a measured temperature below 0°C indicates frozen soil. Based on regression analyses and temperature measurements, an equation is developed to relate the air temperature with the temperature at any depth z.

Although the frost depth determined by this method is approximate due to the soil's isothermal behavior, especially during the spring thaw period, a good indication of the pavement frost depth may be obtained (Atkins 1989). A more accurate measurement of the frost depth may be obtained by using soil resistivity probes. Resistivity probes rely on the measurement of electrical resistance between conductors mounted along a cylindrical probe to determine where the soil is frozen and where it is thawed (see Figure A-6).

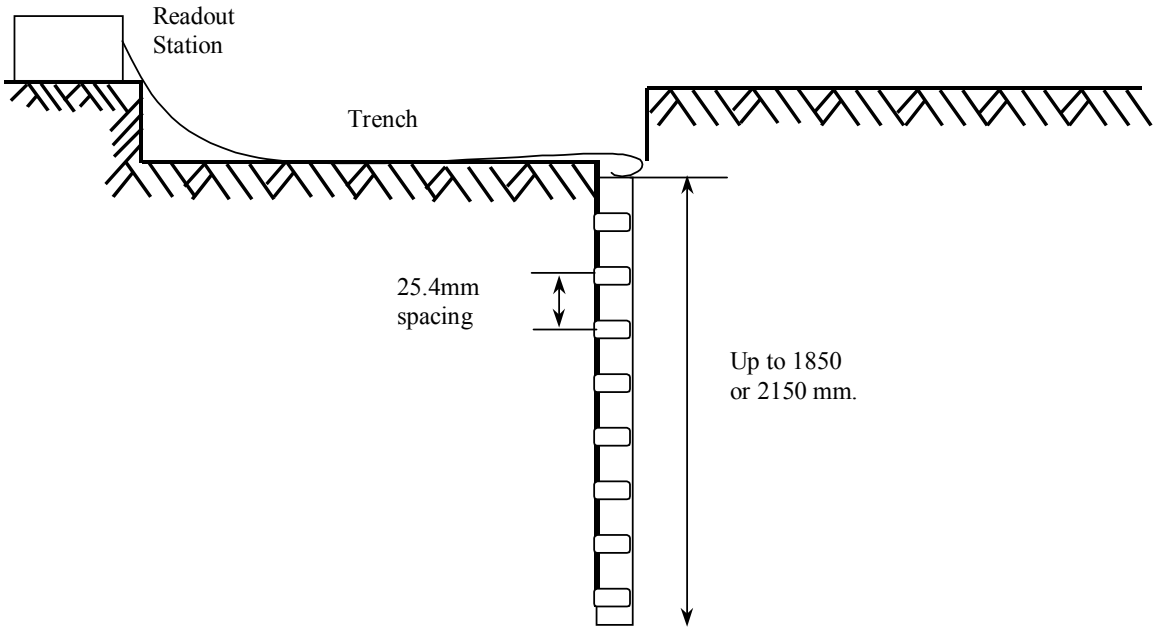

Figure A-6. Resistivity Probe

This concept is based on the wide difference between the volume resistivity of frozen soil (from 500,000 up to several million Ω) and thawed soil (normally 20,000 to 50,000 Ω). Frost penetration is determined by making sequential resistance measurements between adjacent pairs of electrodes down the resistivity probe and documenting at what depth the resistance goes from a high to a low value. It is not even necessary to actually read the resistance**,** since a readout circuit may be used in which voltage measurements for each probe section may be ratioed to a fixed 100KΩ resistor located in the output circuit. Resistivity probes are usually made from PVC rods. The bare copper rings on the gauge must be in actual electrical contact with the soil particles over the entire surface area to insure that a representative resistivity value is obtained. The spacing between the copper rings must be uniform for the entire length of the probe to maintain constant dimensions in the governing equation:

$$R = \rho L / A \qquad (A.32)$$

where

R = measured resistance;

ρ = resistivity of the soil;

A = surface area of the bare copper rings; and

L = spacing between the bare copper rings.

As long as the area (A) and the length (L) are constant, the only variable in the resistance measurement is the resistivity of the soil; thus, the resistance is a true indicator of the frozen or thawed condition. The length of the gauge varies with the application, but should be at least 300mm below the expected frost depth to ensure that the resistivity measurement of unfrozen ground is available throughout the entire freeze/thaw season.

A.6.1.6 Thermocouple

Many instruments, including thermocouples and thermistors, are used to measure temperature. Thermocouples have numerous advantages over thermistors and other temperature transducers (ASTM 1981):

- Thermocouples are inherently simple, being only two wires joined together at the measuring ends.
- The cost of this type of sensor is very low and can be manufactured in-house.
- A thermocouple can cover a wide range of temperatures, and its output is reasonably linear over the major operation range.
- A thermocouple is not subject to self-heat, as is the case with most temperature transducers.

The most commonly used thermocouples are identified by letter designations assigned by the Instrument Society of America (ISA). These types of thermocouples used in most of the engineering applications are as follows:

- Type T: Copper (+) versus constantan (-).
- Type S: Platinum-ten percent rhodium (+) versus platinum (-).
- Type E: Nickel-ten percent chromium (+) versus constantan (-).

- Type J: Iron (+) versus constantan (-).
- Type R: Platinum-thirteen percent rhodium (+) versus platinum (-).
- Type K: Nickel-ten percent chromium (+) versus Nickel-5 percent aluminum, silicon (-).

The choice of a type of thermocouple depends on the working environment, the seeded temperature range, and the required accuracy. For example, thermocouples of type T are resistant to corrosion in moist atmospheres, and are suitable for subzero temperature measurements. They have an upper temperature limit of 370°C, and can be used in a vacuum or inert atmosphere. The expected limits of error with type T-thermocouples are within ± 1% of the measured temperatures in degree Celsius. However, this accuracy is usually expected to decrease if measured temperatures are below the ice point (ASTM 1986).

A.6.2 Recent Instrumented Pavement Research

In recent years, several projects have investigated pavement response to mechanical and environmental loading. Since interlayer systems are mainly evaluated through stretches of highways in the existing infrastructure, the performance of the different interlayer can be quantified, but the contributing mechanism is rarely understood. The main instrumented project initiated to investigate the effectiveness of interlayer systems is the Bedford project in Virginia. The following sections present a quick overview of the most notable instrumented pavement research.

A.6.2.1 The Minnesota Road (MnRoad)

The Minnesota test road (MnRoad), operating from 1993, consists of two pavements, a 4.8-km roadway for high-volume traffic research, and a 4km closed loop for low traffic research (Metcalf 1996). The two pavements are divided into forty 60m heavily instrumented test sections. More than 4500 instruments are embedded in the pavement sections. Soil pressure cells and strain gauges are used at different depths to measure

horizontal and vertical pavement responses. Environmental factors, such as moisture, temperature, and frost depth, are also continuously monitored. The main purpose of this facility is to verify and improve existing pavement models, learn more about the factors that affect pavement response and performance, and develop new pavement models that will allow the building and maintenance of more economical roadways. To date, the contribution of this project appears mainly on the evaluation of different backcalculation software and the selection of the most appropriate routines for the Minnesota Department of Transportation.

A.6.2.2 The Nevada Wes Track

The Wes Track, which started operations in 1995 and closed in 1999, is a 2.8-km oval closed track with 26 experimental HMA pavement sections. The major objective of the Wes Track project was the evaluation of HMA pavement performance and its variation with different design parameters (binder content, gradation, density, etc.). The instrumentation of the 26 sections was primarily environmental. Although a few HMA strain gauges were also installed, their service life was less than six months. The testing stopped in this facility after complete failure of most of the test sections, which were not cost-effective to repair for further investigation.

A.6.2.3 The NCAT Pavement Test Track

The National Center of Asphalt Technology (NCAT) pavement test track, which is located in Auburn, Alabama, is an extension of the Wes Track pavement facility. Construction started in late 1998, and truck loading was undertaken in the summer of 2000. This facility consists of a 2.8-km oval closed track divided into 46 different pavement sections. All sections have the same design, but differ in the mix design for the surface layer. The main objective of this facility is to apply a design-life loading on different pavement sections over a period of two years to investigate the performance of different SuperPave™ mixes. Only environmental sensors were embedded in the

pavement structure during construction (time domain reflectometers for moisture measurement and thermistors for temperature measurement).

A.6.2.4 The Bedford Project

This project is the only instrumented pavement facility that includes interlayer systems (geosynthetics). Nine instrumented secondary road test sections were constructed as part of the realignment of Routes 757 and 616 in Bedford County, Virginia. Each test section was 15m long. Three test sections were constructed using geogrid, three with geotextile, and three were non-stabilized. The pavement sections were instrumented with pressure cells, HMA strain gauges, soil moisture sensors (gypsum blocks), and thermocouples. Foil-type strain gauges were used to monitor the changes in horizontal strain at the bottom of the geotextile. All instrumentation, cabling, and data acquisition facilities were located underground. The data acquisition system was triggered by truck traffic passing over piezoelectric sensors. The main objective of this project was to evaluate the effectiveness of geosynthetics as separators and reinforcement for granular materials. A design procedure was also developed based on the measured pavement responses (Bhutta 1998).

A.7 THE VIRGINIA SMART ROAD

The Virginia Smart Road, located in Southwest Virginia, is a unique, state-of-the-art, full-scale research facility for pavement research and evaluation of Intelligent Transportation Systems (ITS) concepts, technologies, and products. The Virginia Smart Road is the first facility of its kind to be built from the ground up with its infrastructure incorporated into the roadway. When completed, the Virginia Smart Road will be a 9.6-km connector highway between Blacksburg and I-81 in Southwest Virginia, with the first 3.2km designated as a controlled test facility. The pavement research facility at the Virginia Smart Road allows the testing of various hypotheses on pavement material performance and characteristics. Its infrastructure is unique in many aspects, including the fact that all pavement layers are instrumented for monitoring the effects of loading

and the environment; additionally, pavement materials can be tested under different environmental conditions using the All Weather Testing facility. This facility allows the simulation of different types of weather conditions using 76 snow towers to simulate snow and rain conditions that occur naturally. The towers produce snowfalls of up to 100 mm/hr, similar to blizzard snowfalls, and rainfall of up to 50 mm/hr. The towers can rotate 360°, and can pivot toward the roadway to adjust for prevailing wind conditions (see Figure A-7).

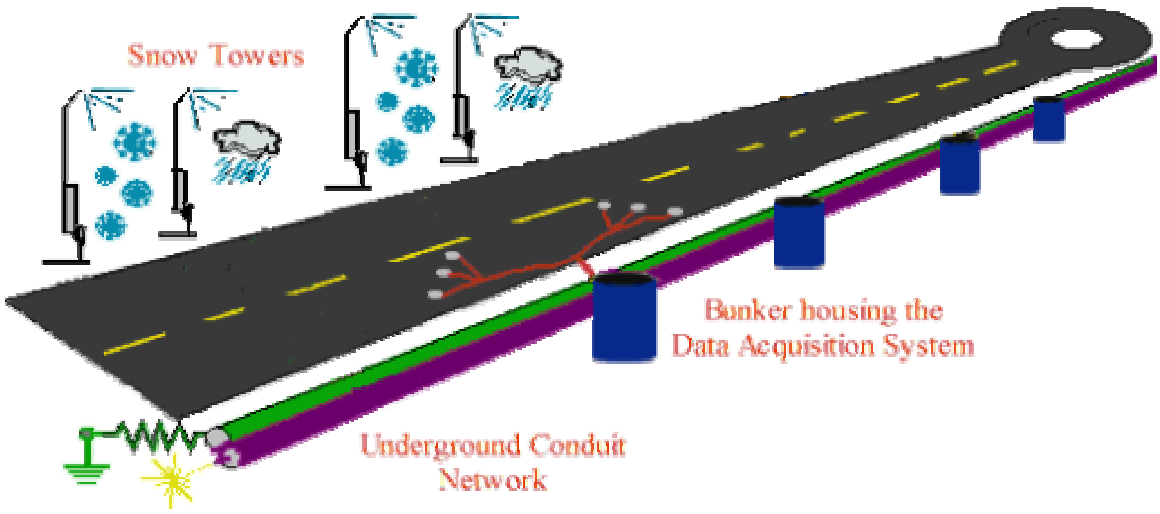

Figure A-7. Schematic of the Virginia Smart Road

An underground conduit network with manhole access (bunker) was used for installing a power and data network without creating a safety hazard to vehicles that may leave the normal roadway. The underground conduit network consists of a conduit for low power, two 100-mm conduits with four inner-ducts for communications, and several spare conduits for future expansion. The conduits are placed on both sides of the roadway to provide access to power and communications without running bare wires across the roadway. The conduit network also routes power to the bunker, where all pavement instruments are connected to the data acquisition system.

Current power grid design issues include minimizing the potential electromagnetic interference between high current-carrying lines and sensitive data

acquisition equipment. A fiber-optic network serves as the backbone information network for the test bed. It is used for the transmission of digital data originating from on-site data acquisition systems. The pavement test road includes flexible pavement test sections and a continuously reinforced rigid pavement. The first 10m length of each section was left as a transition area to accommodate changes in material placement between adjacent sections with different designs. The second 10m length is the instrumented portion. The third 10m length was designated for falling weight deflectometer (FWD) testing, followed by a 10m length designated for ground penetrating radar (GPR) calibration. The instrumented areas of each two sections are designed to be adjacent to each other (separated by the twenty meter-long transition area), so that the instrument wires in the two sections are connected to one bunker (which houses the data acquisition system). Therefore, six data acquisition systems were needed for the twelve flexible pavement sections. The accurately surveyed bunkers are used as reference points. All instruments were surveyed prior to being placed.

The Virginia Smart Road project has been made possible through the cooperative efforts of several federal and state organizations, including the Virginia Department of Transportation (VDOT), The Virginia Transportation Research Council, the Federal Highway Administration, and Virginia Tech.

A.7.1 Flexible Pavement Design

The flexible pavement segment of the Virginia Smart Road test facility includes twelve heavily instrumented flexible pavement sections, shown in Table A-4. Section length varies between 76 and 117 meters. Seven of the twelve sections are located on a fill, while the remaining five sections are located in a cut. Different layers are used in each section (all designations and mix designs are in accordance with VDOT specifications). The different layers are as follows:

- Wearing surface: Seven types of wearing surface are used (SM-9.5A, SM-9.5A with high laboratory compaction, SM-9.5D, SM-9.5E, SM-12.5D, SMA-12.5, and open-graded friction course (OGFC)). Five of these seven are SuperPave™

mixes. All of the mixes, with the exception of the OGFC, were constructed at 38mm-thick. The OGFC was constructed at 19mm-thick.

- Base HMA layer: BM-25.0 at different thickness, ranging from 100 to 244mm.
- Three sections have the SuperPave™ SM9.5A fine mix placed under the BM-25.0 to examine the benefits of such a design on reducing fatigue cracking.
- Open-graded drainage layer (OGDL): Out of the twelve sections, three sections were built without OGDL. Seven sections were treated with asphalt cement, and two were treated with Portland cement. The thickness of this layer is kept constant at 75mm throughout the project.
- Cement Stabilized Subbase: 21-A cement-stabilized layer is used in 10 sections at a thickness of 150mm.
- Subbase layer: 21-B aggregate layer was placed over the subgrade at different thickness with and without a geosynthetic.

As the construction of the first phase of this project is complete (3.2km controlled test facility), the Virginia Smart Road is currently used as a test facility by allowing only controlled traffic loading to pass over the different pavement sections. Among the twelve heavily instrumented sections, four sections were built with different interlayer products (see Table A-4). Three different types of steel reinforcement have been installed over the complete length of section I, and over 50m of the length of section L.

A.7.2 Pavement Instrumentation

The instrument selections and locations were chosen to facilitate understanding of how steel reinforcement could contribute to the pavement system. The transverse and longitudinal strains were monitored at different layer interfaces. Vertical stresses were measured at different locations, which were chosen with respect to the interlayer system. Table A-5 illustrates the different instruments used in sections I and L.

Table A-4. Pavement Design at the Virginia Smart Road

Section	Station Starts	Station Ends	Bunker Station	Lane Length (m)	Surface 38mm	BASE BM-25.0 (mm)	BASE SM-9.5A (mm)	OGDL (mm)	21A Aggr. Cem. Stab. (mm)	21B Aggr. (mm)	Pave. Thick. (mm)	Fill/ Cut
A	102.67	103.71	103.71	104	SM-12.5D	150	0	75	150	175	588	Fill
B	103.71	104.61	103.71	90	SM-9.5D	150	0	75	150	175/ GT	588	Fill
C	104.61	105.48	105.48	87	SM-9.5E	150	0	75	150	175/ GT	588	Fill
D	105.48	106.65	105.48	117	SM-9.5A	150	0	75	150	175/ GT	588	Fill
Bridge	106.65	107.70										
E	107.70	108.46	108.46	76	SM-9.5D	225	0	0	150	75/ GT	488	Fill
F	108.46	109.40	108.46	94	SM-9.5D	150	0	0	150	150	488	Fill
G	109.40	110.30	110.30	90	SM-9.5D	100	50	0	150	150/ GT	488	Fill
H	110.30	111.20	110.30	90	SM-9.5D	100	50	75	150	75	488	Cut/ Snow
I	111.20	112.18	112.18	98	SM-9.5A*	100/RM	50	75	150	75	488	Cut/ Snow
J	112.18	113.10	112.18	92	SM-9.5D	225	0	75	0/MB	150	488	Cut/ Snow
K	113.10	113.96	113.96	86	OGFC+SM-9.5D	225/SR	0	75 (Cement)	0	150	488	Cut/ Snow
L	113.96	115.00	113.96	104	SMA-12.5+	150/RM	0	75 (Cement)	150	75	488	Cut/ Snow

* High lab compaction

SR: Stress Relief Geosynthetic; GT: Woven Geotextile/ Separator; RM: Reinforcing Mesh; MB: Moisture Barrier

Table A-5. Instruments Used at the Virginia Smart Road in Sections I and L

Instrument Type	Picture	Applications	Main Properties
Pressure Cell	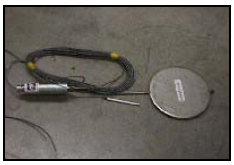	▪ Vertical Stress	▪ Diaphragm cell gauge ▪ Temperature resistance
HMA Strain Gauge		▪ Dynamic and static transverse and longitudinal strains in bounded layers	▪ Low stiffness ▪ Temperature resistant ▪ Good durability
Aggregate Strain Gauge		▪ Dynamic and static transverse and longitudinal strains in granular layers	▪ Suitable for large aggregate size ▪ Very stiff
Time Domain Reflectometer CS610	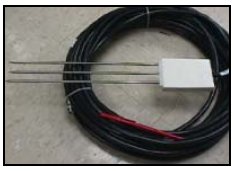	▪ Moisture content in granular layers	▪ Output is reflection coefficient versus time
Time Domain Reflectometer CS615		▪ Moisture content in granular layers	▪ Output is frequency ▪ Laboratory calibrated
Vibrating Wire		▪ Static strains in granular layers	▪ Durable ▪ Relies on frequency ▪ Accurate
Resistivity Probe		▪ Frost depth penetration	▪ 600 and 900mm in length ▪ Area is constant
Thermocouple		▪ Temperature measurement	▪ In-House manufactured ▪ T-type thermocouple

Six different types of instruments were used in these two sections: pressure cells, H-type strain gauges, vibrating wire strain gauges, aggregate strain gauges, time domain reflectometer probes (CS610 and CS615), thermocouples, and resistivity probes.

A.7.2.1 Pressure Cell Gauges

RST pressure cells were selected for this project. This type of pressure gauge consists of two circular steel plates welded together around their rims to create a cell approximately 150mm or 225mm in diameter and 12.5mm-thick (Aspect Ratio = 0.05). The space between the plates is liquid-filled. The fluid has a boiling point of 197°C, which is higher than the HMA placement temperature in order to prevent expansion of the gauge during installation. A steel tube connects the liquid to an electrical pressure transducer. The pressure transducer responds to changes in total stress applied to the material in which the cell is embedded.

Two types of pressure cells are used at the Virginia Smart Road. The first type has a diameter of 150mm and can measure up to 690kPa. These pressure cells have been used in the upper HMA layers of the pavement structure. They have been specially designed to withstand high temperatures during the HMA lay-down. The wires were designed for direct burial, and can withstand temperatures of up to 200°C. The second pressure cell type has a 225mm diameter, and can measure up to 414kPa (see Table A-5). These pressure cells are designed for base layers and subgrades where the stress is lower than the surface and the influence area is greater. The difference in area between the two gauges was designed to address the vertical stress distribution in pavement structures (small influence area at shallow depths and larger influence area at greater depths).

Calibration curves were provided by the manufacturer to convert the measured voltage to vertical stress. Attempts were made to validate the provided calibration curves using an Instron testing machine to subject the cell to vertical loading (the cell was protected with inflatable rubber membranes during loading). Some differences were found between the two approaches, as the applied load by the testing machine was purely static and did not consider the dynamic nature of the applied load in real pavement, while the manufacturer's approach used a pressurized chamber. That resulted in a shift in the

calibration relation. It was therefore decided to follow the calibration factors supplied by the manufacturer. The stiffness effect of the gauge was later addressed after installation by field calibration and theoretical verification.

A.7.2.2 H-type Strain Gauges

Dynatest Past-II-AC H-type strain gauges were used to measure the dynamic transverse and longitudinal strains in all HMA layers (see Table A-5). The gauge has an effective length of 102mm with two flanges, 75mm-long and 15mm-wide. The strain gauge has a cross-section area of only $50mm^2$, which requires an extremely low "strain force" of 0.11N/microstrain. The average modulus of the cell body is as low as 2.2GPa due to the special properties of the cell materials. This low stiffness avoids the reinforcement of the pavement layers by the presence of the gauge.

This type of strain gauge is completely embedded in a strip of glass-fiber reinforced epoxy, a material with a relatively low stiffness and high flexibility and strength. Each end of the epoxy strip is securely fastened to a stainless steel anchor to ensure proper mechanical coupling to the HMA material after installation. The PAST transducer (1/4 bridge) has a resistance of 120 ohms, and a gauge factor of 2.0. It can be incorporated into a full bridge setup with up to 12V excitation voltage. The gauge can measure up to 1500 microstrains (tension or compression), with an expected fatigue life of 10^6 cycles.

To validate the manufacturer calibration, a caliper has been designed and manufactured at Virginia Tech to simulate the expected range of strain that the H-type strain gauge may be exposed to. The designed caliper is capable of applying a uniformly static or dynamic tension/compression force to the gauge by means of a screw shaft that moves in both directions without applying torsion or bending to the gauge. A sensitive micrometer head ($2x10^{-4}$mm) was connected to the system to measure the exact amount of applied displacement to the gauge. By changing the fixing apparatus, this caliper was suitable for any type of strain gauge. It was used for the three main types of strain gauges used in this project. Figure A-8 illustrates the in-house manufactured caliper.

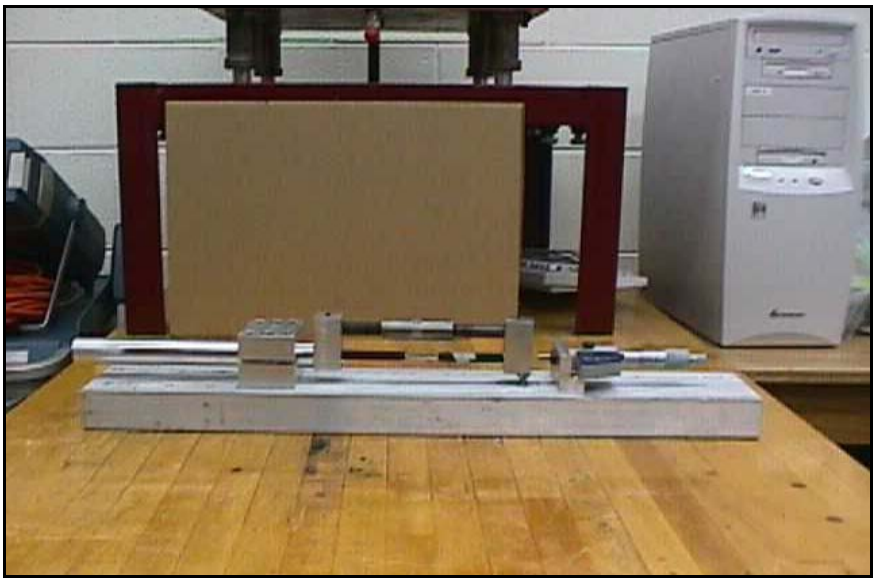

Figure A-8. Strain Gauge Caliper

A.7.2.3 Thermocouples

T-type thermocouples were used at the Virginia Smart Road to provide an accurate measurement of heat flow inside the pavement system. The performance of this type of thermocouple has been excellent in previous projects performed at Virginia Tech. Taking into account service life, field installation, and price, in house T-type thermocouples were manufactured for this project.

Each thermocouple operation was checked for the expected operating temperature range. The expected limits of error with the T-type thermocouples are within ± 1% of the measured temperatures in degrees Celsius. However, this accuracy is usually expected to decrease if the measured temperatures fall below the ice point (ASTM 1986). As they were manufactured to full-field-required length, no lead wire splicing was required.

A.7.2.4 Time Domain Reflectometry

Subbase and subgrade moisture contents were measured using time domain reflectometers (TDRs). Time domain reflectometer probes consist of multiple stainless

steel rods (two or more) that are inserted in the host material. The soil moisture content is evaluated by sending a pulsed signal through the host material and examining its reflection. Since the amplitude and frequency of the reflected signal are based on the dielectric properties of the host material, the measurements can be related to soil moisture content (the dielectric constant of dry aggregates ranges from four to eight, depending on the mineral compositions, and the dielectric constant of wet aggregates can reach up to twenty). This conversion can rely on equations provided by the manufacturer (with an accuracy of ±2%). However, greater accuracy can be achieved by developing calibration equations from comparisons between moisture contents using the TDR and gravimetric methods (oven drying).

Two types of TDR probes were used in the Virginia Smart Road: the traditional CS610 and the newly developed CS615 (see Figure A-9). The CS610 water content reflectometer consists of three conducting rods that are 300mm in length. Output from the CS610 TDR is usually displayed as voltage or as a reflection coefficient versus time. To obtain the volumetric moisture content from the probe output, use can be made of the universal equation proposed by Topp et al. (1980):

$$\theta_v = -5.3 \times 10^{-2} + 2.92 \times 10^{-2} \varepsilon_a - 5.5 \times 10^{-4} \varepsilon_a^2 + 4.3 \times 10^{-6} \varepsilon_a^3 \quad \text{(A.33)}$$

where

θ_v = volumetric moisture content (percent); and

ε_a = apparent dielectric constant that is defined as follows (Topp et al. 1980):

$$\varepsilon_a = \left(\frac{ct}{l} \right)^2 \quad \text{(A.34)}$$

where

c = velocity of an electromagnetic wave in free space (3×10^8m/s);

l = length of the TDR transmission line (m); and

t = two-way travel time of the electromagnetic wave as measured by the TDR system (sec).

(a) (b)

Figure A-9. Configuration of the TDR Probes Used at the Virginia Smart Road: (a) CS610 and (b) CS615

The CS615 consists of two parallel conducting rods that are also 300mm in length. Output from the CS615 is usually displayed as frequency. The output from the probes can be converted into volumetric moisture content by using the equations provided by the manufacturer (with an accuracy of ±2%). Greater accuracy can be achieved by developing calibration equations from comparisons between moisture contents using the TDR method and gravimetric methods. Such calibration equations were developed for the 21B granular materials used at the Virginia Smart Road (Diefenderfer et al. 2000). The CS615 probes were calibrated for a volumetric moisture content ranging from one to 20%. Different calibration equations (second and third order) were developed from the obtained laboratory data (Diefenderfer et al. 2000):

$$\theta_v = -0.6816t^2 + 1.7907t - 0.9692 \quad \text{(A.35)}$$

$$\theta_v = 5.6821t^3 - 17.267t^2 + 17.767t - 6.0495 \quad \text{(A.36)}$$

where

t = time in msec; and

θ_v = volumetric moisture content.

The obtained coefficients of determination (R^2) for the developed equations ranged between 0.97 and 0.99, which is an acceptable level of accuracy for the range of measurement of interest (from one to 20%). Although the results from the two probes are

correlated, this study only presents the results of the CS615 probe, as it provides continuous data, and can be easily connected to a data acquisition system.

A.8 NON DESTRUCTIVE TECHNIQUES

This study makes use of different non-destructive techniques to monitor the performance and construction effectiveness of the different interlayer systems installed at the Virginia Smart Road. Two techniques were regularly used: ground penetrating radar and falling weight deflectometer. This section presents a quick overview of the two techniques.

A.8.1 Ground Penetrating Radar

Ground penetrating radar (GPR) was periodically used to monitor water movement in the pavement sections at the Virginia Smart Road and to identify any significant changes in the pavement system profile. Two GPR types (900 MHz ground-coupled and 1 GHz air-coupled) were used in this project; see Figure A-10. This technique is based on sending electromagnetic waves through the surveyed structure and then analyzing the reflected signal (Loulizi et al. 1999). The velocity of electromagnetic waves in a material can be estimated as follows:

$$v = \frac{c}{\sqrt{\epsilon_r}} \tag{A.37}$$

where

v = speed of propagation of the wave (m/s);

c = speed of an electromagnetic wave in free space ($3x10^8$ m/s); and

ϵ_r = relative permittivity (dielectric constant) of the traveling medium.

When an electromagnetic wave travels through two different materials, energy will be reflected and transmitted at the interface. The degree of reflection depends on the relative dielectric constants of the two materials. This is approximated as follows:

$$r = \frac{\sqrt{\epsilon_{r1}} - \sqrt{\epsilon_{r2}}}{\sqrt{\epsilon_{r1}} + \sqrt{\epsilon_{r2}}} \quad \text{(A.38)}$$

where

r = degree of reflection;

ϵ_{r1} = relative permittivity of the first layer; and

ϵ_{r2} = the relative permittivity of the second layer.

Air Coupled System (1GHz)

Ground Coupled System (900MHz)

Figure A-10. Ground Penetrating Systems Used at the Virginia Smart Road

Equations (A.37) and (A.38) are considered the basis for the interpretation of GPR data. From Equation (A.37), one can calculate either the unknown thickness of a given layer (knowing the dielectric constant) or the dielectric constant of a given layer (knowing the exact thickness). On the other hand, Equation (A.38) is used to determine if moisture accumulation exists in a given layer by monitoring the changes in the amplitude of the reflected signal. Free water has a very high dielectric constant (81) compared to construction materials (3-8).

A.8.2 Falling Weight Deflectometer

Falling weight deflectometer (FWD) is a deflection test, in which a force pulse is applied to the pavement system by dropping a weight on a specially designed set of springs. This produces an impact load with a duration of 25-30msec, which corresponds to a wheel velocity of 80km/hr for the upper layer (Ullidtz 1987). Surface deflections are measured and recorded by seven (or more) geophones at various distances from the loading point; see Figure A-11.

A number of deflection basin parameters (e.g. radius of curvature, spreadability, deflection ratio, etc.), which are functions of deflection values at one or more sensors, were introduced to check the structural integrity of in-service pavements. Most of these parameters reflect one simple idea: the greater the deflection(s), the weaker the pavement system. Currently, this system is widely used at the network level to diagnose the structural integrity of in-service pavement.

Figure A-11. Falling Weight Deflectometer System

A more sophisticated analysis may be accomplished by using the resulting deflection basin, which consists of backcalculating the layer moduli using the multi-layer elastic theory and giving the thickness and Poisson's ratio of each layer. A composite modulus,

known as the surface modulus, may also be evaluated for the entire pavement structure. This modulus, which can be used as an overall representation of the pavement stiffness, is defined as follows (Rada et al. 1994):

$$E_{comp} = \frac{p\, a_c{}^2 (1-\mu^2)\, C}{def\ r} \tag{A.39}$$

where

E_{comp} = modulus of composite pavement structure;

p = contact pressure applied by the FWD;

μ = Poisson's ratio;

def = measured deflection at a given radial distance r;

a_c = load plate radius; and

C = a deflection constant defined as follows:

$$C = 1.1 \log\left(\frac{r}{a_c}\right) + 1.15 \tag{A.40}$$

A.9 REFERENCES

AASHTO, American Association of State Highway and Transportation Official. (1986). *Guide for design of pavement structures*, Washington, D.C.

Abd El Halim, A. O., Haas, R., and Phang, W. A. (1983). "Geogrid reinforcement of asphalt pavements and verification of elastic theory." *Transportation Research Record 949*, Transportation Research Board, Washington, D.C., 55-65.

Al-Qadi, I. L., Brandon, T. L., Valentine, R. J., Lacina, B. A., and Smith, T. E. (1994). "Laboratory evaluation of geosynthetic-reinforced pavement sections." *Transportation Research Board 1439*, Transportation Research Board, Washington, D.C., 25-31.

Al-Qadi, I. L., and Loulizi, A. (1999). "Using GPR to evaluate the effectiveness of moisture barriers in pavements." *Structural Faults and Repair 99*, 8th International Conference, Forde, M. C., editor, London, England, July 13-15.

ASTM, American Society for Testing and Materials. (1986). "Manual on the use of thermocouples in temperature measurement." ASTM Special Technical Publication 470A, Library of Congress Catalog Card Number: 73-90277.

Atkins, R. T. (1989). "Determination of frost penetration by soil resistivity measurements." *Symposium on the State-of-the-Art of Pavement Response Monitoring Systems for Roads and Airfields*, sponsored by U.S. Army Cold Regions Research and Engineering Laboratory, Report 89-23, 87-100.

Barksdale, R. D., Brown, S. F., and Chan, F. (1989). "Potential benefits of geosynthetics in flexible pavements." NCHRP Report 315, Transportation Research Board, Washington, D.C.

Barksdale, R. D. (1991). "Fabrics in asphalt overlays and pavement maintenance." NCHRP Report 171, Transportation Research Board, Washington, D.C.

Bekaert. (1989). "Corrosion of galvanized wire reinforcement in asphalt coatings." Prepared by J. Moens (Research and Development), Report No. 046040/002/89.

Beckham, W. K., and Mills, W. H. (1935). "Cotton-fabric-reinforced roads." *Engineering News Record*, Vol. 114, No. 14.

Bhutta, S. (1998). "Mechanistic-empirical pavement design procedure for geosynthetically stabilized flexible pavements." PhD thesis, Dept. of Civil Engineering, Virginia Polytechnic Inst. and State University, Blacksburg, VA.

Brown, S. F., Thom, N. H., and Sanders, P. J. (2001). "A study of grid reinforced asphalt to combat reflection cracking." *J. Assoc. Paving Technologists*, Vol. 70, 543-571.

Brownridge, F. C. (1964). "An evaluation of continuous wire mesh reinforcement in bituminous resurfacing." *Proc., Annual Meeting of the Association of Asphalt Paving Technologists*, Vol. 33, Dallas, TX, 459-501.

Busching, H. W., Elliott, E. H., and Reyneveld, N. G. (1970). "A state-of-the-art survey of reinforced asphalt paving." *Proc., Annual Meeting of the Association of Asphalt Paving Technologists*, Vol. 39, Kansas City, MO, 766-797.

Button, J. W., and Lytton, R. L. (1987). "Evaluation of fabrics, fibers and grids in overlays." *Proc., 6th International Conference on Structural Design of Asphalt Pavements*, Vol. 1, Ann Arbor, MI, 925-934.

Button, J. W. (1989). "Overlay construction and performance using geotextiles." *Transportation Research Record 1248*, Transportation Research Board, Washington, D.C., 24-33.

BRCC, Belgian Road Research Center. (1995). "Evaluation of mesh track projects." Report EP 3709 (French Version), Brussels, Belgium.

BRRC, Belgian Road Research Center. (1998). "Design of overlaid cement concrete pavements reinforced with Bitufor® traffic loading." Research report EP5035/3544, Brussels, Belgium.

BRCC, Belgian Road Research Center. (1999). "The design of concrete pavements reinforced with a glass fibre grid (comparison between the anticracking system Bitufor and Trasyn)." Report EP 5242/2415, Brussels, Belgium.

Buttlar, W. G., Bozkurt, D., and Dempsey, B. J. (2000). "Cost-Effectiveness of paving fabrics used to control reflective cracking." *Transportation Research Record 1730*, Transportation Research Board, Washington, D.C.

Cancelli, A. (1999). "In-ground test for geosynthetic reinforced flexible paved roads." *Proc., Geosynthetics '99*, Boston, MA, 863-878.

Carmichael III, R. F., and Marienfeld, M. L. (1999). "Synthesis and literature review of nonwoven paving fabrics performance in overlays." *Transportation Research Board 1687*, Transportation Research Board, Washington, D.C., 112-124.

Chen, H. J., and Frederick, D. A. (1992). "Interlayers on flexible pavements." *Transportation Research Record 1374*, Transportation Research Board, Washington, D.C.

Coni, M., and Bianco, P. M. (2000). "Steel reinforcement influence on the dynamic behavior of bituminous pavement." *Proc., 4th International RILEM Conference – Reflective Cracking in Pavements*, E & FN Spon, Ontario, Canada, 3-12.

Davis, N. M. (1960). "A field study of methods of preventing reflection cracks in bituminous resurfacing of concrete pavements." Report No. 12, University of Toronto, Toronto, Ontario.

Diefenderfer, B. K., Al-Qadi, I. L., and Loulizi, A. (2000). "Laboratory calibration and field verification of soil moisture content using time-domain reflectometry." *Transportation Research Record 1699*, Transportation Research Board, Washington, D.C., 142-150.

Donna, H. S. (1993). "Crack-reduction pavement-reinforcement glassgrid." Colorado Department of Transportation, prepared in cooperation with the U.S. Department of Transportation, Federal Highway Administration.

Donovan, E. P., Al-Qadi, I. L., and Loulizi, A. (2000). "Optimization of tack coat application rate for a geocomposite membrane used on bridge decks." *Transportation Research Record 1740*, Transportation Research Board, Washington, D.C., 143-150.

Epps, A., Harvey, J. T., Kim, Y. R., and Roque, R. (2000). "Structural requirements of bituminous paving mixtures." *Transportation in the New Millennium*, Transportation Research Board, Washington, D.C.

Francken, L., and Vanelstraete, A. (1992). "Interface systems to prevent reflective cracking." *Proc., 7th International Conference on Asphalt Pavements*, International Society for Asphalt Pavements, Nottingham, UK, 45-60.

Francken, L. (1993). "Laboratory simulation and modeling of overlay systems." *Proc., 2nd International RILEM Conference – Reflective Cracking in Pavements*, E & FN Spon, Liege, Belgium, 75-99.

Graf, B. and G. Werner. (1993). "Design of asphalt overlay – fabric system against reflective cracking." *Proc., 2nd International RILEM Conference – Reflective Cracking in Pavements*, E & FN Spon, Liege, Belgium, 159-168.

Hozayen, H., Gervais, M., Abd El Halim, A. O., and Haas, R. (1993). "Analytical and experimental investigations of operating mechanisms in reinforced asphalt pavements." *Transportation Research Record 1388*, Transportation Research Board, Washington, D.C., 80-87.

Huang, Y. H. (1993). *Pavement analysis and design*, 1st ed., Prentice-Hall, NJ.

Huges, C. S., and McGhee, K. H. (1973). "Results of reflective crack questionnaire survey." Report No. VHRC 72-R25, Virginia Highway Research Council.

Huhtala, M., and Pihlajamaki, J. (1992). "Strain and stress measurements in pavements." *Proc., Conference Sponsored by the U.S. Army Cold Regions Research and Engineering Laboratory* - Road and airport pavement response monitoring systems, Federal Aviation Administration, West Lebanon, New Hampshire, American Society of Civil Engineers, 229-243.

Huhtala, M., Alkio, R., Pihlajamaki, J., Pienimaki, M., and Halonen, P. (1992). "Behavior of bituminous materials under moving wheel loads." *Proc., Annual Meeting of the Association of Asphalt Paving Technologists*, Vol. 65, Baltimore, MD, 422-443.

Huhtala, M., Pihlajamaki, J., and Halonen, P. (1997). "Pavement response due to dynamic axle loads." *Proc., 8th International Conference on Asphalt Pavements*, University of Washington, Seattle, WA, Vol. 1, 471-485.

Kanninen, M. F., and Popelar, C. H. (1985). *Advanced fracture mechanics,* Oxford University Press, Inc., New York, NY.

Kennepohl, G., Kamel, N., Walls, J., and Hass, R. C. (1985). "Geogrid reinforcement of flexible pavements design basis and field trials." *Proc., Annual Meeting of the Association of Asphalt Paving Technologists*, Vol. 54, San Antonio, TX, 45-75.

Kim, J., and Hjelmstad, K. (2000). "Three-dimensional finite element analysis of multi-layered systems: compressive nonlinear analysis of rigid airport pavement systems." *Center of Excellence for Airport Pavement Research*, COE Report No. 10, University of Illinois at Urbana-Champaign, Illinois.

Koerner, R. M. (1994). *Designing with geosynthetics*, 3rd ed., Prentice Hall, NJ.

Komatsu, T., Kikuta, H., Yoshinobu, T., and Muramatsu, E. (1998). "Durability assessment of geogrid-reinforced asphalt concrete." *Geotextiles and Geomembranes*, Vol. 16, 257-271.

Krarup, J. (1992). "Instrumentation for a full-scale pavement test in the Danish road testing machine." *Proc., Conference Sponsored by the U.S. Army Cold Regions Research and Engineering Laboratory* - Road and airport pavement response monitoring systems, Federal Aviation Administration, West Lebanon, New Hampshire, American Society of Civil Engineers, 96-111.

Li, N., Haas, R., and Kennepohl, G. (1992). "Geosynthetics in asphalt pavements: structural, materials, design and performance considerations." *Proc., 37th Annual Conference of Canadian Technical Asphalt Association*, Victoria, British Columbia, 224-242.

Loulizi, A., Al-Qadi, I. L., Bhutta, S. A., and Flintsch, G. W. (1999). "Evaluation of geosynthetics used as separators." *Transportation Research Record 1687*, Transportation Research Board, Washington, D.C., 104-111.

Lytton, R. L. (1989). "Use of geotextiles for reinforcement and strain relief in asphalt concrete." *Geotextiles and Geomembranes*, Vol. 8, 217-237.

Majidzadeh, K., Luther, M. S., and Skylut, H. (1982). "A mechanistic design procedure for fabric-reinforced pavement systems." *Proc., 2nd International Conference on Geotextiles*, Las Vegas, NV.

Makela, H., Lehtonen, J., and Kallio, V. (1999). "Finnish experiences in preventing frost damages of roads by using steel meshes." *Geotechnical Engineering for Transportation Infrastructure*, Rotterdam, Finland, 1335-1340.

Marienfeld, M. L., and Baker, T. L. (1999). "Paving fabric interlayer as a pavement moisture barrier." *Transportation Research Circular E-C006*, Transportation Research Board, Washington, D.C.

Majidzadeh, K. (1976). "A laboratory investigation of the use of Petromat for optimization of pavement performance." Ohio State University, Sponsored by Phillips Petroleum Company.

Measurement Group Inc. (1994). "Student manual for strain gauge technology." Raleigh, NC.

Metcalf, J. B. (1996). "Application of full-scale accelerated pavement testing." NCHRP Report 235, Transportation Research Board, Washington, D.C.

Molenaar, A. A., Heerkens, J. C., and Verhoeven, J. H. (1986). "Effects of stress absorbing membrane interlayers." *Proc., Annual Meeting of the Association of Asphalt Paving Technologists*, Vol. 55, Clear Water Beach, FL, 453-481.

Monismith, C. L., and Coetzee, N. F. (1980). "Reflection cracking: analysis, laboratory studies and design considerations." *Proc., Annual Meeting of the Association of Asphalt Paving Technologists*, Vol. 49, Louisville, KY, 268-313.

Nejad, F. M., and Small, J. C. (1996). "Geogrid reinforcement of pavements." *Proc., 7th Australia New Zealand Conference on Geomechanics: Geomechanics in a Changing World*, Adelaide, South Australia, 129-133.

Owusu-Antwi, E. B., Khazanovich, L, and Titus-Glover, L. (1998). "A mechanistic-based model for predicting reflective cracking in AC overlaid pavements." *Transportation Research Record 1629*, Transportation Research Board, Washington, D.C., 234-241.

Paris, P. C., and Erdogan, F. A. (1963). "Critical analysis of crack propagation laws." *Transactions of the ASME, Journal of Basic Engineering*, Series D, No. 3, 528-533.

Rada, G. R., Richter, C. A., and Jordahl, P. (1994). "SHRP's layer moduli backcalculation procedure." *Nondestructive Testing of Pavements and Backcalculation of Moduli*, ASTM STP 1198, Harold L. Von Qunitas, Albert J. Bush, III, and Gilbert Y. Baladi, Eds, American Society for Testing and Materials, Philadelphia, 38-52.

Richard, T. H., and Robertson, A. W. (1983). "The determination of single and mixed mode stress intensity factors for engineering components of practical interest." *Fracture Mechanics in Engineering Practice*, P. Stanley, Ed, Applied Science Publishers LTD, London, 1-32.

Rigo, J. M. (1993). "General introduction, main conclusions of 1989 conference on reflective cracking in pavements, and future prospects." *Proc., 2nd International RILEM Conference – Reflective Cracking in Pavements*, E & FN Spon, Liege, Belgium, 3-20.

Roberts, F. L., Kandhal, P. S., Brown, E. R., Lee, D. and Kennedy, T. W. (1996). "Hot mix asphalt materials, mixture design, and construction." 2nd ed., Napa Education Foundation, Lanham, Maryland, 532.

Schapery, R. A. (1982). "Models for damage growth and fracture in nonlinear particulate composites." *Proc., 9th US Congress of Applied Mechanics*, ASME.

Selig, E. T. (1989). "In-situ stress measurements." *Symposium on the State-of-the-Art of Pavement Response Monitoring Systems for Roads and Airfields*, sponsored by U.S. Army Cold Regions Research and Engineering Laboratory, Report 89-23, 162-168.

Senstad, P. (1994). "Increased bearing capacity and increased pavement service life using steel reinforcements in asphalt pavements." *Proc., 4th International Conference on the Bearing Capacity of Roads and Airfields*, Minneapolis, Minnesota, Vol. 2, 1331-1343.

Smith, R. D. (1983). "Laboratory testing of fabric interlayers for asphalt concrete paving: Interim report." *Transportation Research Record 916*, Transportation Research Board, Washington, D.C., 6-18.

Smith, R. D. (1984). "Laboratory investigation of fabric interlayer for asphalt concrete pavement." Final report, FHWA/CA/TL-84-06, California Department of Transportation.

Steinberg, M. L. (1992). "Geogrid as a rehabilitation remedy for asphaltic concrete pavements." *Transportation Research Record 1369*, Transportation Research Board, Washington, D.C., 54-62.

Steen, E. R. (2000). "Road maintenance: technical aspects regarding the choice of geosynthetics." *Proc., 4th International RILEM Conference – Reflective Cracking in Pavements*, E & FN Spon, Ontario, Canada, 507-516.

Tabatabaee, N., and Sebaaly, P. (1990). "State-of-the-art pavement instrumentation." *Transportation Research Record 1260*, Transportation Research Board, Washington, D.C., 246-255.

Tons, E., Bone, A. J., and Roggeveen, V. J. (1961). "Five-year performance of welded wire fabric in bituminous resurfacing." *Highway Research Board Bulletin 290*, Washington, D.C., 43 -80.

Torry, A. C., and Sparrow, R. W. (1967). "The influence of the diaphragm flexibility on the performance of an earth pressure cell." *Journal of Scientific Instruments*, Vol. 44, 781-785.

Ullidtz, P. (1987). *Pavement analysis*, Elsevier Science, New York, NY.

Ullidtz, P. (1989). "State-of-the-art stress, strain and deflection measurements." *Symposium on the State-of-the-Art of Pavement Response Monitoring Systems for Roads and Airfields*, sponsored by U.S. Army Cold Regions Research and Engineering Laboratory, Report 89-23, 148-161.

Ullidtz, P. (1998). *Modelling flexible pavement response and performance*, 1st ed., Polyteknisk Forlag, Denmark.

Vanelstraete, A., and Francken, L. (1993). "Numerical modeling of crack initiation under thermal stresses and traffic loads." *Proc., 2nd International RILEM Conference – Reflective Cracking in Pavements*, E & FN Spon, Liege, Belgium, 136-145.

Vanelstraete, A., Leonard, D., and Veys, J. (2000). "Structural design of roads with steel reinforcing nettings." *Proc., 4th International RILEM Conference – Reflective Cracking in Pavements*, E & FN Spon, Ontario, Canada, 56-67.

Vanelstraete, A., and Francken, L. (2000). "On site behavior of interface systems." *Proc., 4th International RILEM Conference – Reflective Cracking in Pavements*, E & FN Spon, Ontario, Canada, 517-526.

Veys, J. (1996). "Steel reinforcement for the prevention of cracking and rutting in asphalt overlays." *Proc., 3rd International RILEM Conference – Reflective Cracking in Pavements*, E & FN Spon, Maastricht, The Netherlands, 402-411.

Vogelzang, C. H., and Bouman, S. R. (1992). "In-situ stress and strain measurements in dynamically loaded asphalt pavement structures." *Proc., Conference Sponsored by the U.S. Army Cold Regions Research and Engineering Laboratory* - Road and airport pavement response monitoring systems, Federal Aviation Administration, West Lebanon, New Hampshire, American Society of Civil Engineers, 245-259.

White, T. D. (1989). "Instrumentation and pavement design." *Symposium on the State-of-the-Art of Pavement Response Monitoring Systems for Roads and Airfields*, sponsored by U.S. Army Cold Regions Research and Engineering Laboratory, Report 89-23, 2-8.

Zanten, R. V. (1986). *Geotextiles and geomembranes in civil engineering,* J. Wiley, New York, NY.